Fuel 106 (2013) 30–50

Contents lists available at SciVerse ScienceDirect

Fuel

journal homepage: www.elsevier.com/locate/fuel

Review article

A review of fire processes modeling of combustible materials under external heat flux

Long Shi *, Michael Yit Lin Chew

Department of Building, National University of Singapore, Singapore 117566, Singapore

ARTICLE INFO

Article history:
Received 14 March 2012
Received in revised form 11 December 2012
Accepted 14 December 2012
Available online 5 January 2013

Keywords:
Pyrolysis
Combustion
Mechanical behaviors
Fire processes
One-dimensional modeling

ABSTRACT

One-dimensional model is fundamental to two- or three-dimensional modeling of combustible materials, which can be classified into wood, non-charring polymer, charring polymer and intumescent polymer according to their characteristics. Four fire processes are involved in fire development, such as thermal process, physical process, chemical process and failure process. Consideration of all four fire processes for these combustible materials is significant to modeling accuracy and application fields. Therefore, the state of the art of one-dimensional modeling describing all four fire processes of woods, non-charring polymers, charring polymers and intumescent polymers under external heat flux was reviewed. A summary of typical considerations in previous one-dimensional models was provided, including heat conduction, pyrolysis, production of gas volatiles, volume change, water evaporation, internal gas pressure, properties of permeability and porosity, and mechanical behaviors. Empirical models and critical data of fire processes were also collected for modeling input. This paper can provide a guide to one-dimensional modeling and build basis for two- and three-dimensional modeling.

Contents

* Corresponding author. Tel.: +65 83818700.
E-mail addresses: shilong@mail.ustc.edu.cn, shilong@nus.edu.sg (L. Shi).

0016-2361/$ - see front matter © 2013 Published by Elsevier Ltd.
http://dx.doi.org/10.1016/j.fuel.2012.12.057

Nomenclature

A	pre-exponential frequency factor (1/s)
c	concentration (mol/m^3)
C_p	specific heat capacity (J/kg/K)
E	activation energy (kJ/mol)
E	young's modulus (Pa)
f	shrinkage factor (–)
k	rate of reaction (1/s)
L	thickness of specimen (m)
m	mass (kg)
$\dot{m}''$	mass flux (kg/m^2/s)
M	molecular weight (kg/mol)
P	pressure (MPa)
$\dot{q}''$	external heat flux (w/m^2)
Q	heat of reaction (J/kg)
r	radial distance from the center (m)
R	universal gas constant (J/mol/k)
t	time (s)
T	absolute temperature (K)
u	velocity (m/s)
x	cartesian coordinate (m)
X	moisture content (–)
y	yield (g/g)
Y	species mass fraction (–)

Greek symbols

α	conversion of reaction (–)
ΔA	unit cross-section area (m^2)
Δh	specific enthalpy of materials (J/kg)
Δx	control volume width (m)
ε	emissivity of materials (–)
ϕ	porosity (–)
γ	permeability (m^2)
λ	thermal conductivity (W/m/K)
μ	dynamic viscosity (kg/m/s)
ρ	density (kg/m^3)
σ	compression/tension (Pa)

Subscripts and superscripts

a	active material between virgin material and char
ave	average
bound	bound water
c	char
C	carbon
CO	carbon monoxide
CO_2	carbon dioxide
convec	convection process
desorp	desorption process
evap	evaporation process
f	final conditions
g	gas phase
H_2O	water
i	species i of solid or reaction i
l	liquid water/phase
N_2	nitrogen gas
O_2	oxygen gas
s	solid phase
sat	fiber saturation point
soot	soot
t	tar
v	virgin material
0	ambient conditions

Abbreviations

ABS	acrylonitrile butadiene styrene
CO	carbon monoxide
CO_2	carbon dioxide
CH_4	methane
GRP	glass rein-forced plastics
HDPE	high-density polyethylene
HIPS	high-impact polystyrene
H_2O	water
LDPE	low-density polyethylene
N_2	nitrogen gas
O_2	oxygen gas
PA	polyamide (nylon)
PBT	poly(butylenes terephthalate)
PC	polycarbonate
PE	polyethylene
PET	poly(ethylene terephthalate)
PMMA	poly(methylmethacrylate)
PP	polypropylene
PS	polystyrene
PVC	poly(vinyl chloride)

1. Introduction

Four species of combustible materials have been investigated in previous one-dimensional modeling, including wood, non-charring polymer, charring polymer, and intumescent polymer. According to chemical compositions, woods can be classified into hardwood and softwood. Hardwood and softwood have the similar percentage of cellulose, but hardwood have a little higher hemicelluloses and less lignin than those of softwood [1]. Non-charring polymers such PMMA, HIPS, and HDPE have no or very few residues after burning. And both charring polymers and intumescent polymers leave char after burning. Intumescent polymers melt and degrade to form a viscous fluid, and they undergo expansion due to produce of large amounts of gas. Polymers such as PET goes through shrinkage under external heat flux, but PVC, PC, and carbon phenolic undergo expansion [2–4]. It is difficult to develop a model which can describe all four species of combustible materials as modeling differences exist among these combustible materials. Different approaches are needed for the modeling of these combustible materials [5]. For example, non-charring materials can be modeled using theory similar to flammable liquids. Pyrolysis of charring polymer is a complex interplay of chemistry, heat and mass transfer. They must be modeled in terms of a pyrolysis front penetrating into the materials with an increasing surface temperature and without a well-defined steady state. And the modeling of intumescent polymer is the most challenge one because of irregular expanding char. A summary of modeling differences among these combustible materials are listed in Table 1.

Fire processes of combustible materials under external heat flux can be concluded into four types [6]: thermal process, chemical process, physical process, and failure process. To describe these fire processes, some typical considerations were taken in previous models, including heat conductivity, pyrolysis, production of gas volatile, volume change, internal pressure, water evaporation, properties of permeability and porosity, and mechanical behaviors. It is critical to explore these considerations as they could greatly improve modeling accuracy and expand application fields.

Table 1
A summary of modeling differences among combustible materials.

Items	Wood	Non-charring polymer	Charring polymer	Intumescent polymer
Pyrolysis reaction[a]	– Two-steps	– One-step	– Multi-step	– Multi-step
Residue	– Char	– Very few or no residue	– Char	– Expanded char
Volume change	– Shrinkage	– Shrinkage	– Shrinkage or expansion	– Expansion
Transition temp.	– N/A	– Glass temperature melting temperature	– Glass temperature melting temperature	– Glass temperature melting temperature
Thermal properties	– Consider as linear	– Change before and after transition temperature	– Change before and after transition temperature	– Change before and after transition temperature
Solid phase	– Char layer pyrolysis layer virgin wood	– Pyrolysis layer virgin polymer	– Char layer pyrolysis layer virgin polymer	– Char layer expanding layer virgin polymer
Grain	– Across or along	– N/A	– N/A	– N/A

[a] The pyrolysis reaction is summarized based on the consideration of previous models.

Progresses on fire processes modeling have been made gradually. In 1965, a one-dimensional mathematical model was developed to predict thermal process of wooden dowel by Tinney [7]. Heat transfer was described by Fourier conduction equation with a heat-source term. And pyrolysis reaction was expressed by a first-order Arrhenius equation. Later in 1972, exhausted gas volatile was considered by Kung [8]. Gas volatiles were regarded as flowing out immediately after production. In 1987, gaseous permeability of wood was measured and used to simulate drying process by Perre [9]. In 1990, Aerts and Ragland [10] developed a model considered gas phase, consisting of oxygen, hydrocarbons, CO, CO_2 and water vapor. In 1992, McManus and Springer [11] developed a model which described responses of carbon phenolic under mechanical loading. Subsequently, many works have been done on one-dimensional modeling of combustible materials under external heat flux [12–22].

Fig. 1 shows a statistics of considerations in previous one-dimensional models. It is noticed that most of the models have focused on woods, and few models focused on non-charring and intumescent polymers. Considerations such heat conductivity, pyrolysis are essential to fire processes modeling. However, modeling accuracy and application fields are challenged because of the absence of considerations such as volume change, water evaporation, and mechanical behaviors.

To improve modeling accuracy and expand the applications fields, efforts are still needed to be put in several aspects. Firstly, some critical data are needed to be collected. For example, modeling results are quite sensitive to kinetic data [21]. Collection of kinetic data for both woods and polymers is critical to modeling accuracy. Modeling accuracy is also hampered when thermal properties were considered as temperature independent. Critical data or empirical models describing temperature dependent thermal properties are needed to be collected as well. Secondly, some considerations are not often taken in previous models and needed to be explored, such as volume change, internal pressure, water evaporation, properties of permeability and porosity, mechanical behaviors. Lastly, descriptions of all four fire processes for both woods and polymers are significant to improve modeling accuracy. And an integrated model which can describe different species of combustible materials is critical for fire processes modeling.

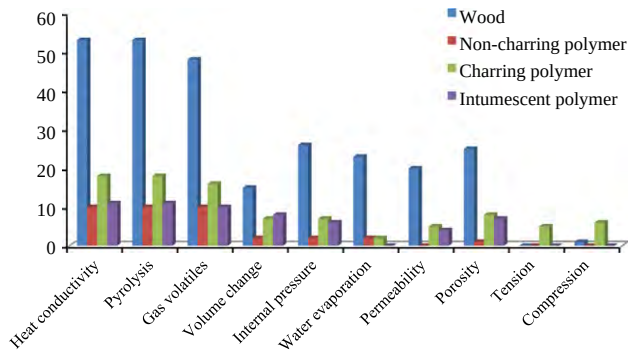

Fig. 1. Statistics of considerations in previous one-dimensional models.

This paper presents a critical review of one-dimensional modeling of combustible materials under external heat flux, including woods, non-charring polymers, charring polymers, and intumescent polymers. A summary of typical considerations in previous one-dimensional models was provided, including heat conduction, pyrolysis, generation of gas volatiles, volume change, water evaporation, internal gas pressure, properties of permeability and porosity, and mechanical behaviors. Empirical models and critical data of fire processes are also collected. This paper can provide a guide to one-dimensional modeling and build basis for two- and three-dimensional modeling.

2. Fire processes

2.1. Thermal process

Thermal process is essential to one-dimensional modeling of combustible materials. At the beginning, Fourier's law was used to described heat transfer inside solid phase [7]. Surface radiation, convection heat loss were ignored. Thermal conductivity was also considered temperature independent. Later, thermal properties were described in modeling by interpolation between char and virgin materials [8,23,24]. As the development of experimental conditions, temperature dependent thermal properties such as thermal conductivity, specific heat capacity, surface absorptivity were obtained and used in modeling [25–27]. Some typical models showed the progress of thermal process description, which will be provided as follows.

In 1965, a one-dimensional mathematical model was developed for the combustion of small wooden dowels heated externally by Tinney [7]. Heat transfer was described by Fourier conduction equation, including a heat-source term:

$$\rho C_p \frac{\partial T}{\partial t} = \lambda \left(\frac{\partial^2 T}{\partial r^2} + \frac{1}{r} \frac{\partial T}{\partial r} \right) - Q \frac{\partial \rho}{\partial t} \quad (1)$$

The surface was assumed to heat evenly, and heat entered inside from the surface to the center. And the center was assumed as inert.

Later in 1972, Kung [8] developed a model to describe wood slabs heated externally. Convection heat of gas volatiles and endothermicity of pyrolysis reactions were considered in this model, which was expressed as:

Table 2
Surface absorptivities of combustible materials dependent on temperature.

Name	Blackbody emitter temperature (K)						Flame	Solar
	1000	1500	2000	2500	3000	3500		
Alaskan cedar	–	–	–	0.44	–	–	0.76	0.36
Ash	–	–	–	0.46	–	–	0.76	0.36
Balsa	–	–	–	0.41	–	–	0.75	0.35
Birch	–	–	–	0.47	–	–	0.77	0.39
Cottonwood	–	–	–	0.48	–	–	0.76	0.40
Mahogany	–	–	–	0.49	–	–	0.76	0.52
Mansonia	–	–	–	0.47	–	–	0.76	0.51
Maple	–	–	–	0.49	–	–	0.76	0.44
Oak	–	–	–	0.56	–	–	0.77	0.49
Redgum	–	–	–	0.52	–	–	0.77	0.56
Redwood	–	–	–	0.51	–	–	0.77	0.55
Spruce	–	–	–	0.45	–	–	0.76	0.35
White pine	–	–	–	0.49	–	–	0.76	0.43
Masonite	–	–	–	0.52	–	–	0.75	0.61
PP	0.87	0.83	0.78	0.74	0.70	0.68	0.86	0.62
PS (clear)	0.75	0.60	0.46	0.35	0.28	0.22	0.78	0.095
PS (white)	0.86	0.75	0.63	0.53	0.45	0.40	0.88	0.29
Polyurethane thermoplastic	0.92	0.89	0.83	0.77	0.72	0.68	0.93	0.62
PVC (clear)	0.81	0.65	0.49	0.38	0.30	0.24	0.85	0.15
PVC (gray)	0.90	0.90	0.89	0.89	0.89	0.89	0.91	0.89
PVC/acrylic (gray, rolled)	0.88	0.87	0.86	0.85	0.84	0.83	0.88	0.81
PVC/acrylic (red cast)	0.91	0.90	0.89	0.88	0.87	0.86	0.92	0.86
Rubber (Buna-N)	0.92	0.93	0.93	0.93	0.93	0.93	0.92	0.94
Rubber (Butyl IIR)	0.92	0.93	0.94	0.94	0.95	0.95	0.92	0.95
Rubber (natural, gum)	0.88	0.82	0.76	0.72	0.69	0.68	0.89	0.69
Rubber (neoprene)	0.91	0.92	0.93	0.93	0.93	0.93	0.91	0.94
Rubber (silicone)	0.79	0.66	0.58	0.54	0.52	0.53	0.79	0.62

$$\rho C_{ps}\frac{\partial T}{\partial t}=\frac{\partial}{\partial x}\left(\lambda\frac{\partial T}{\partial x}\right)+m''_g\frac{\partial \Delta h_g}{\partial x}+\frac{\partial \rho}{\partial t}\left(Q-\frac{\rho_v}{\rho_v-\rho_f}\Delta h_a+\frac{\rho_f}{\rho_v-\rho_f}\Delta h_c+\Delta h_g\right) \quad (2)$$

The first three term describe the effects of transient and spatial temperature changes and convection heat of gas volatiles. The last term is the endothermicity of pyrolysis reactions.

For boundary conditions, exposed surface receives external heat flux, while the bottom was assumed as inert. The boundary conditions were expressed as:

$$\begin{cases} -\lambda\frac{\partial T}{\partial x}=\dot{q}'', & x=0 \\ \frac{\partial T}{\partial x}=0, & x=L \end{cases} \quad (3)$$

Predicted temperature by Kung's model is much higher than practice when surface heat losses of convection and radiation were ignored. This problem was solved in Kansa's model [28], which were expressed as:

$$\begin{cases} -\lambda\frac{\partial T}{\partial x}=\varepsilon\dot{q}''-\varepsilon\sigma\left(T^4-T_0^4\right)-h_{convec}(T-T_0), & x=0 \\ \frac{\partial T}{\partial x}=0, & x=L \end{cases} \quad (4)$$

where σ is Stefan–Bolzmann constant, 5.6704×10^{-8} W/m^2 K^4.

Thermal properties may change as temperature rises. In kung's model, thermal conductivity was expressed by interpolation between virginal wood and char:

$$\lambda=\frac{\rho-\rho_c}{\rho_v-\rho_c}\lambda_v+\frac{\rho_v-\rho}{\rho_v-\rho_c}\lambda_c \quad (5)$$

In this equation, if $\rho\to\rho_v$, $\lambda=\lambda_v$; and if $\rho\to\rho_c$, $\lambda=\lambda_c$. However, this description was not so accurate to describe the thermal properties when comparing to the direct measurement.

The use of temperature dependent thermal properties may largely increase the modeling accuracy. Temperature dependent thermal properties were later used by Fan et al. [27], which are expressed by:

$$\begin{cases} \lambda=\lambda_0+p_1(T-T_0) \\ C_p=C_{p0}+p_2(T-T_0) \end{cases} \quad (6)$$

where p_1 and p_2 are coefficients.

Absorptivity of combustible materials is a very important thermal property for boundary conditions. Some models considered it as temperature independent and modeling results were affected. Temperature dependent absorptivities of combustible materials are then gathered for modeling input, shown in Table 2 [21,29,30]. Experiments were used to measure absorptivities of blackbody heat source. Solar radiation was considered as a 6000 K heat source, and tungsten as a 2500 K heat source. Absorptivities of combustible materials at specific temperature can be obtained by interpolation.

2.2. Chemical process

2.2.1. Pyrolysis reaction

Different pyrolysis reactions exist for woods and polymers. For woods, pyrolysis process can be expressed by a two-steps reaction. Virginal woods change into gas, tar and char during pyrolysis reactions. Then the tar changes into gas and char at the same time. Although the pyrolysis reactions of some polymers are very complicated, they can be simply considered that they change into gas and char directly, namely one-step reaction. Pyrolysis reaction scheme of wood and polymer is shown in Fig. 2. The dash line for polymer represents non-charring polymers as they produce no or very few char.

Studies on woods' pyrolysis reactions have never stopped. Several types of models have been developed previously:

- The first type is a two-steps reaction, which can be seen in Fig. 2.
- Another type of model was developed under the consideration that woods consist of three main chemical components, such as cellulose, hemicelluloses and lignin [31–35]. Individual pyrolysis reaction for these three chemical components was used in

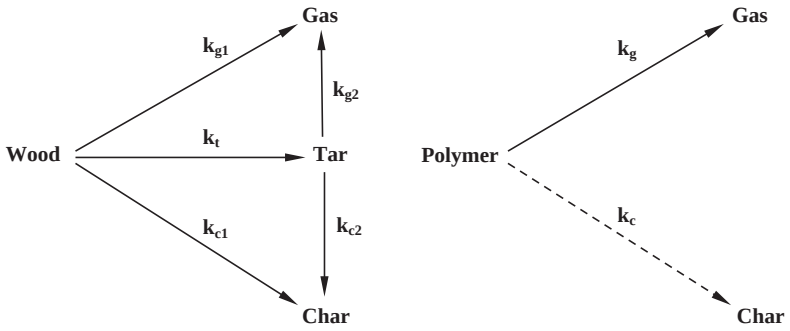

Fig. 2. Pyrolysis reaction scheme of wood and polymer.

modeling as they show different characteristics during their pyrolysis reactions. The pyrolysis reactions of woods were then regards as the mixture of these three chemical components.

- A different pyrolysis model was developed by Kilzer–Broido [31,36]. In this model, wood was pyrolyzed through two paths. One was an endothermic tar producing reaction and the other was an intermediate solid producing reaction which was assumed to have a zero heat of pyrolysis. The intermediate solid, corresponding to dehydrocellulose in this model, was decomposed into char and gas during an exothermic reaction.
- According to above models, Park et al. [31] developed a model which is similar to the first model. The difference is that woods change into intermediate solid first before changing into char.

Pyrolysis reactions in Fig. 2 can be described by Arrhenius law. For woods, virgin material changes into gas volatiles, tar, and char synchronously. And polymer changes into gas and char directly. Total mass loss depends on all these pyrolysis reactions, which can be given as:

$$\begin{cases} \frac{\partial m_s}{\partial t} = km_0 = (k_{g1} + k_t + k_{c1})m_0, & \text{Wood} \\ \frac{\partial m_s}{\partial t} = km_0 = (k_g + k_c)m_0, & \text{Polymer} \end{cases} \tag{7}$$

For individual pyrolysis reaction, mass loss can be given as:

$$\frac{\partial m_i}{\partial t} = -k_i m_0 \tag{8}$$

where i is the pyrolysis reaction; and subscripts of $g1$, t, $c1$, $g2$ and $c2$ represent pyrolysis reactions of wood, and g and c for polymer, shown in Fig. 2.

Reaction rate k is governed by the Arrhenius Law:

$$k_i = A_i \left(\frac{m_s - m_f}{m_0}\right)^n \exp\left(-\frac{E_i}{RT}\right) \tag{9}$$

Pyrolysis reactions of woods and polymers are also affected by concentration of oxygen. Tihay et al. [37] investigated the influence of oxygen concentration on kinetics of cellulose. It was gained that increasing the oxygen concentration tends to shift the pyrolysis and char oxidation to lower temperature and to raise the maximum mass loss rate. Martin-Gullon et al. [38] conducted experiments on pyrolysis reactions of PET with different proportions of oxygen. Results showed that the higher the oxygen presence, the earlier the char consumption finishes. Different pyrolysis stages were obtained when polymer under different atmosphere conditions [39]. Influence of oxygen on pyrolysis reactions can be expressed by the following form:

$$\frac{\partial \alpha}{\partial t} = A \exp\left(-\frac{E}{RT}\right) P_{O_2}^m (1-\alpha)^n \tag{10}$$

where P_{O_2} is the partial oxygen pressure, Pa; m is reaction order with respect to oxygen; and α is conversion of reaction, which can be defined as:

$$\alpha = \frac{m_0 - m}{m_0 - m_f} \tag{11}$$

Table 3 shows a summary of kinetic data of different species of combustible materials. Activation energy and pre-exponential frequency factor were obtained by experiments. Most of the pyrolysis reactions were expressed by one-step kinetic equation. Temperature ranges of related pyrolysis reactions are provided. Although many experiments have been taken, it is noticed that few data are obtained for the production of gas volatiles and tar.

2.2.2. Combustion of char

Combustion of char has always played an important role in modeling of combustible materials under external heat flux. A large number of studies have been done on combustion of char. Saastamoinen et al. [59–63] have put a lot of effects on simulations for both circulating fluidized-bed combustion and pulverized fuel combustion, considering the gasification, oxygen concentration, pressure, moisture, etc. A one-dimensional steady state model has been developed to analyzed combustion of biomass char in circulating fluidized bed by Kaushal et al [64]. This model included different sub-models that are linked together to describe the overall combustion process, such as hydrodynamic and reaction sub-models. Refs. [65–71] have provided a comprehensive review on combustion of char.

Reactions of carbon and oxygen have been extensively investigated for coal char, but still present aspects that are poorly understood [66]. However, the most widely used treatment is called global power-law:

$$C + O_2 \rightarrow CO/CO_2, \quad k = A_0 \exp(-E/RT) P_{O_2}^n \tag{12}$$

where P_{O_2} is the partial pressure of oxygen; and A_0, E are kinetic data representing char oxidation rate. A summary of these kinetic data can be found in Ref. [66].

As the productions of CO and CO_2 are significant, studies have been done on the ratio CO/CO_2 during char combustion process. Arthur [72] conducted experiments on combustion of artificial graphite and coal char using flow method. It was found that the CO/CO_2 ratio was independent of burning time, air velocity (when temperature is lower than 900 °C) and initial partial pressure of oxygen in the range 38–190 mmHg. But this CO/CO_2 ratio increased exponentially with temperature in the range 480–900 °C, appeared to be uniquely determined by the temperature.

Tognotti et al. [73] investigated the ratio CO_2/CO from oxidation of Spherocarb char for temperatures up to 1670 K. It was obtained that CO_2/CO ratio was proportional to the oxygen partial pressure raised to a power of 0.21. The CO_2/CO ratios produced by heterogeneous oxidation of carbons was summarized by an exponential relation:

$$CO_2/CO = A \exp\left(\frac{B}{T}\right) \tag{13}$$

Table 3
A summary of kinetic data of different species of combustible materials.

Material type	Reference	Material	Experimental condition	Temp. range (K)	Kinetic constants
Softwood	Samolada and vasalos [40]	Fir wood	Isothermal	673–773	$k_{g1} + k_t = 2.40 \times 10^4 \exp(-94/RT)$
	Wagenaar et al. [41]	Pine	TGA[a]	553–673	$k_{c1} = 3.05 \times 10^7 \exp(-125/RT)$
				773–873	$k_t = 9.28 \times 10^9 \exp(-149/RT)$
					$k_{g1} = 1.11 \times 10^{11} \exp(-177/RT)$
					$k = 1.4 \times 10^{10} \exp(-150/RT)$
	Chan et al. [42]	Pine	–	–	$k_{c1} = 1.08 \times 10^7 \exp(-121/RT)$
					$k_t = 2 \times 10^8 \exp(-133/RT)$
					$k_{g1} = 1.3 \times 10^8 \exp(-140/RT)$
	Liu and Fan [43]	Nanmu	TGA	435–568	$k = 5.53 \times 10^8 \exp(-116.57/RT)$
	n=2			568–623	$k = 1.99 \times 10^{24} \exp(-290.53/RT)$
				623–728	$k = 5.91 \times 10^5 \exp(-109.37/RT)$
				728–787	$k = 2.30 \times 10^{21} \exp(-320.37/RT)$
	Liu and Fan [43]	Paulownia	TGA	455–571	$k = 7.64 \times 10^{11} \exp(-149.0/RT)$
				571–631	$k = 1.44 \times 10^{18} \exp(-215.21/RT)$
				631–671	$k = 3.90 \times 10^{20} \exp(-287.32/RT)$
				671–775	$k = 7.42 \times 10^{48} \exp(-645.17/RT)$
Hardwood	Thurner and Mann [44]	Oak sawdust	Isothermal	573–673	$k_{g1} = 1.43 \times 10^4 \exp(-88.6/RT)$
					$k_t = 4.13 \times 10^6 \exp(-112.7/RT)$
					$k_{c1} = 7.38 \times 10^5 \exp(-106.5/RT)$
					$k_{g1} + k_t = 1.73 \times 10^6 \exp(-106.5/RT)$
					$k = 2.49 \times 10^6 \exp(-106.5/RT)$
	Di Blasi and Branca [45]	Beech	–	573–708	$k_{g1} + k_t = 1.5 \times 10^{10} \exp(-149/RT)$
					$k_{c1} = 3.3 \times 10^6 \exp(-112/RT)$
					$k_{g1} = 4.4 \times 10^9 \exp(-153/RT)$
					$k_t = 1.1 \times 10^{10} \exp(-148/RT)$
	Gorton and Knight [45]	Hardwood	Isothermal	677–822	$k = 1.483 \times 10^6 \exp(-89.52/RT)$
	Ward and Brashlaw [45]	Wild cherry	Isothermal	538–593	$k = 1.19 \times 10^{12} \exp(-173.7/RT)$
	Nunn et al. [46]	Sweet gum	Non-isothermal	600–1400	$k_{g1} + k_t = 3.338 \times 10^5 \exp(-69/RT)$
	Font et al. [45]	Almond shell	–	733–878	$k_{c1} = 2.98 \times 10^3 \exp(-73/RT)$
					$k_t = 5.85 \times 10^6 \exp(-119/RT)$
					$k_{g1} = 1.52 \times 10^7 \exp(-139/RT)$
					$k = 1.885 \times 10^6 \exp(-92.1/RT)$
	Swann et al. [47]	Maple plywood	TGA	353–823	$k = (2.0 \pm 0.33) \times 10^{13} \exp[-(170 \pm 23)/RT]$
			DSC[b]		$k = (1.33 \pm 0.83) \times 10^{11} \exp[-(146 \pm 3)/RT]$
	Liu and Fan [43]	Willow	TGA	446–595	$k = 2.54 \times 10^8 \exp(-118.73/RT)$
				595–658	$k = 2.53 \times 10^{24} \exp(-296.93/RT)$
				658–699	$k = 8.13 \times 10^{14} \exp(-226.56/RT)$
				699–768	$k = 4.41 \times 10^{51} \exp(-711.36/RT)$
Non-charring polymer	Stoliarov et al. [48]	PMMA	TGA	–	$k = 8.5 \times 10^{12} \exp(-188/RT)$
	Stoliarov et al. [48]	HIPS	TGA	–	$k = 1.2 \times 10^{16} \exp(-247/RT)$
	Stoliarov et al. [48]	HDPE	TGA	–	$k = 4.8 \times 10^{22} \exp(-349/RT)$
	Kang et al. [49]	PMMA	TGA (5 K/min)[c]	–	$k = 2.15 \times 10^{16} \exp(-102.461/RT)$
			TGA (10 K/min)		$k = 3.65 \times 10^{19} \exp(-118.494/RT)$
			TGA (15 K/min)		$k = 1.35 \times 10^{17} \exp(-103.822/RT)$
			TGA (20 K/min)		$k = 3.82 \times 10^{23} \exp(-139.502/RT)$
	Bockhorn et al. [50]	PS	Isothermal	633–683	$k = 2.08 \times 10^8 \exp(-95/RT)$
	Carniti et al. [51]	PS	Isothermal	633–693	$k_{g1} + k_{g2} = 6.9 \times 10^{11} \exp(-195/RT)$
	Liu et al. [52]	PS	Isothermal	643–773	$k_{g1} + k_{g2} = 1.16 \times 10^4 \exp(-71.3/RT)$
	Bockhorn and Knumann [53]	PE	–	473–873	$k = 7.2 \times 10^{13} \exp(-259/RT)$ $n = 0.81$[d]
	Urzendowski and Guenther [53]	HDPE	–	673–758	$k = 1.3 \times 10^{21} \exp(-304/RT)$
	Urzendowski and Guenther [53]	LDPE		648–753	$k = 3.1 \times 10^{20} \exp(-290/RT)$
	Ciutacu et al. [54]	PE	Non-isothermal	503–653	$k = 1.8 \times 10^3 \exp(-66.6/RT)$
				653–823	$k = 2.6 \times 10^6 \exp(-121.81/RT)$
	Bockhorn and Knumann [53]	PP	–	473–873	$k = 8.6 \times 10^{11} \exp(-224/RT)$ $n = 0.78$
	Kiang et al. [53]	Isotactic PP	–	661–711	$k = 3.3 \times 10^{13} \exp(-213/RT)$
	Kiang et al. [53]	Atactic PP	–	661–711	$k = 1.4 \times 10^{15} \exp(-234/RT)$
	Sawaguchi et al. [53]	Isotactic PP	–	–	$k = 1.2 \times 10^{10} \exp(-173.9/RT)$
	Sawaguchi et al. [53]	Atactic PP	–	–	$k = 2.0 \times 10^{10} \exp(-171.8/RT)$
	Straus and Wall [53]	PP	–	–	$k = 2.51 \times 10^{14} \exp(-247/RT)$
	Kannan et al. [55]	PP	TGA	673–713	$k = 3.2 \times 10^{15} \exp(-244/RT)$
					$k = 2.2 \times 10^{11} \exp(-188/RT)$
	Kannan et al. [55]	HDPE	TGA	673–723	$k = 1.9 \times 10^{13} \exp(-220/RT)$
	Kannan et al. [55]	LDPE	TGA	673–723	$k = 1.0 \times 10^{15} \exp(-241/RT)$
					$k = 9.8 \times 10^{11} \exp(-201/RT)$
	Fuoss et al. [53]	PS	Isothermal	667	$k = 5.0 \times 10^{24} \exp(-323/RT)$
	Kuroki et al. [53]	PS	–	583–653	$k = 1.8 \times 10^{11} \exp(-152/RT)$
	Madorsky [53]	PS	–	608–628	$k = 9.0 \times 10^{15} \exp(-244/RT)$
	Sato et al. [53]	PS	–	373–873	$k = 3.5 \times 10^{11} \exp(-177/RT)$ $n = 0.75$
	Kannan et al. [55]	PS	TGA	638–673	$k = 3.3 \times 10^{13} \exp(-204/RT)$
	Grammelis et al. [56]	LDPE	–	–	$k = 1.4 \times 10^{28} \exp(-437.1/RT)$
	Grammelis et al. [56]	HDPE	–	–	$k = 4.5 \times 10^{28} \exp(-445.2/RT)$

(*continued on next page*)

Table 3 (*continued*)

Material type	Reference	Material	Experimental condition	Temp. range (K)	Kinetic constants
	Grammelis et al. [56]	PP	–	–	$k = 3.17 \times 10^{24} \exp(-373.4/RT)$
	Grammelis et al. [56]	PS	–	–	$k = 4.0 \times 10^{26} \exp(-414.9/RT)$
Charring polymer	Ciutacu et al. [54]	PA	Non-isothermal	563–793	$k = 1.9 \times 10^{5} \exp(-110.5/RT)$
	Ciutacu et al. [54]	ABS	Non-isothermal	523–743	$k = 2.5 \times 10^{3} \exp(-83.7/RT)$
				743–903	$k = 1.0 \times 10^{8} \exp(-169.9/RT)$
	Grammelis et al. [56]	PA	–	–	$k = 2.83 \times 10^{16} \exp(-256.6/RT)$
Intumescent polymer	Simon [57]	PVC	–	–	$k = 6.61 \times 10^{12} \exp(-162.8/RT)$
					$k = 5.88 \times 10^{12} \exp(-171.9/RT)$
	Bockhorn et al. [58]	PVC	Isothermal	493–623	$k = 2.64 \times 10^{19} \exp(-290/RT)$ $n = 2$
				673–823	$k = 4.19 \times 10^{16} \exp(-260/RT)$ $n = 1.8$
	Ciutacu et al. [54]	PC	Non-isothermal	503–783	$k = 2.8 \times 10^{8} \exp(-151.5/RT)$
				783–893	$k = 3.8 \times 10^{8} \exp(-90.4/RT)$
	Grammelis et al. [56]	PC	–	–	$k = 9.33 \times 10^{20} \exp(-340.7/RT)$

[a] TGA represents thermogravimetric analysis.
[b] DSC represents differential scanning calorimetry.
[c] Value in bracket is the heating rate during experiments.
[d] n is the order of reaction, and no mention means first-order reaction.

where $A = A_0(P_{O_2})^n$, with P_{O_2} in atmospheres, $A_0 = 0.02$; and B is temperature coefficient, which depends on oxygen concentration.

Although one-step global power-law kinetics is popularly used to describe the char combustion up to complete conversion, multi-step models have also been proposed. The additional steps concern the low-temperature devolatilization of char or both devolatilization and combustion of char [66].

Another kinetic expression that has been periodically used to interpret char combustion kinetics is the Langmuir–Hinshelwood expression, which describes competing adsorption and desorption reaction on the char surface [74]. The most commonly applied of this reaction is the two-step Langmuir–Hinshelwood kinetics:

$$\begin{cases} C + O_2 \xrightarrow{k_1} C(O) \\ C(O) \xrightarrow{k_2} CO \end{cases} \tag{14}$$

And the overall burning rate can be expressed by:

$$k = \frac{k_1 k_2 P_{O_2}}{k_1 P_{O_2} + k_2} \tag{15}$$

As the above two models, such as global power-law kinetics and Langmuir–Hinshelwood kinetics, do not provide even the crudest description of the reaction order data, a three-step semi-global kinetics was developed by Hurt and Calo [68]:

$$\begin{cases} C + O_2 \xrightarrow{k_1} 2C(O) \\ C(O) + O_2 \xrightarrow{k_2} CO_2 + C(O) \\ C(O) \xrightarrow{k_3} CO \end{cases} \tag{16}$$

And the overall burning rate can be expressed by:

$$k = \frac{k_1 k_2 P_{O_2} + k_1 k_3 P_{O_2}}{k_1 P_{O_2} + k_3/2} \tag{17}$$

Hurt and Calo [68] made comparisons among above models, such as global power-law, Langmuir–Hinshelwood kinetics, and three-step semi-global kinetics. It was obtained that neither global power-law nor Langmuir–Hinshelwood kinetics were appropriate as general forms for describing char combustion kinetics over entire range of technological interest in temperature and oxygen pressure. And the three-step semi-global kinetics was capable of describing the basic trends in global order, global activation energy, and CO/CO_2 ratio over a wide range of combustion conditions.

More complicated multi-steps model describing char combustion are available, and the details can be seen in Refs. [66,68].

2.2.3. Production of gas volatiles

Many species of gas volatiles are produced when combustible materials is put under external heat flux. Among these gas volatiles, CO is the most significant one because of its characteristic of life-threatening. Roughly two-thirds of all deaths resulting from enclosure fires can be attributed to the presence of CO, which is known to be the dominant toxicant in fire deaths [75].

Two approaches were found to predict production of gas volatiles in previous models. The first approach is to use gas yields directly. And production rates of gas volatiles are connected with mass loss. He and Behrendt [76] used experimental data to predict gas volatiles:

$$\begin{aligned} wood + \Delta h \rightarrow\ & 0.183\,CO + 0.115\,CO_2 + 0.047\,CH_4 + 0.005\,H_2 \\ & + 0.25\,H_2O + 0.2\,tar + 0.2\,char \end{aligned} \tag{18}$$

where Δh is the heat for pyrolysis reactions, J/kg; and coefficients on the right side of equation are yields of products. For example, 0.183 kg CO will be produced after consuming 1 kg wood.

Experiments have been taken to obtain the yields of products of woods, which are listed in Table 4. These yields are dependent on several conditions, such as sample size, temperature, moisture content, atmosphere condition, etc. Experiments in this table are small-scale with particle or powder samples. For a larger sample size, Shi and Chew [77] tested wood slabs under external heat flux in a cone calorimeter, and moisture dependent CO yield was obtained:

$$y_{CO} = (2.6 - 6.9X) \times 10^6 \frac{1}{\dot{q}''^{2.5} \rho L} \quad (10 \leqslant L \leqslant 30) \tag{19}$$

To predict CO production of woods under external heat flux, a model was developed by Shi and Chew [80,81]. In this model, oxidation reactions of both virgin wood and char were included, and CO yields of these two reaction were considered constant even under various external heat flux. Experimental results showed a sharp decrease of CO release rate shortly after ignition and a second peak near the end of experiments [77,82]. Therefore, it was assumed in Shi and Chew's model that the new produced CO during the presence of visible flame change into CO_2 immediately after production. From the comparisons between experiments and modeling, it was noticed that CO release rate of woods under external heat flux can be well predicted by this model.

Another approach to predict production rate of gas volatiles is multi-steps reactions. It is easy to get the chemical formula of polymers. But there is no description on chemical formula of woods.

Table 4
Yields of products of woods.

Material	Sample size	Experimental conditions	Char	Tar	CO	CO_2	H_2O
Sweet gum [46]	Powder of 100 mg	Electrical screen heater reactor, 600–1400 K	0.07	0.46	0.17	0.061	0.051
Pine [42]	1 cm diameter cylinder sample	Moisture content of 0.04–0.05, single-particle Pyrex reactor, heat flux of 167 kW/m^2	0.23	0.44	0.086	0.076	0.15
Almond shell[a] [78]	0.297 -0.50 mm diameter, 30 g	Fluidized bed reactor, nitrogen condition	–	–	0.019–0.038	0.048–0.099	0.16–0.19
Wood [40]	Particle of 2 g	Fluidized bed reactor, temperature range of 400–500 °C	0.272–0.44	–	0.016–0.047	0.045–0.089	–
Sawdust [79]	0.105–0.25 mm diameter	Moisture content of 0.0493, fluidized bed reactor, 350–600 °C, 55% hydrogen and 45% nitrogen by volume	0.018–0.22	Nil	0.028–0.23	0.046–0.19	0.18–0.25
Cellulose [79]	0.105–0.25 mm diameter	Moisture content of 0.0075, fluidized bed reactor, 426–741 °C, nitrogen condition	0.080–0.19	0.29–0.47	0.052–0.27	0.068–0.13	0.13–0.21
Corn stover [79]	0.105–0.25 mm diameter	Moisture content of 0.09, fluidized bed reactor, 450–650 °C, nitrogen condition	0.19–0.46	0.20–0.30	0.025–0.039	0.076–0.098	0.14–0.19

[a] The yields obtained from experiments are dry basis.

Table 5
Average weight percentage of elements of woods.

Element	Hardwoods	Softwoods	Oak bark	Pine bark
C	50.2	52.7	52.6	54.9
H	6.2	6.3	5.7	5.8
O	43.5	40.8	41.5	39.0
N	0.1	0.2	0.1	0.2
S	–	0	0.1	0.1

This problem can be solved by using average weight percentage of each element. Table 5 shows the average weight percentage of each element of woods [83]. To predict production of gas volatiles, Wang [84] assumed that C_xH_y oxidizes to CO and H_2O while intermediate CO oxidizes to CO_2:

$$\begin{cases} \text{Step 1}: \ 1\ \text{kg}\ C_xH_y + \upsilon_1\ \text{kg}\ O_2 \rightarrow 28Y_C/12\ \text{kg CO} + 18(1-Y_C)/2\ \text{kg}\ H_2O \\ \text{Step 2}: \ 1\ \text{kg CO} + \upsilon_2\ \text{kg}\ O_2 \rightarrow (1+\upsilon_2)\ \text{kg}\ CO_2 \end{cases} \tag{20}$$

where Y_C is the mass fraction of carbon in C_xH_y; υ_1 and υ_2 denote the stoichiometric coefficients, which are defined as follow:

$$\upsilon_1 = \frac{32}{12}Y_C + \frac{16}{2}(1-Y_C) - \frac{28}{12}Y_C\upsilon_2, \quad \upsilon_2 = \frac{16}{28} \tag{21}$$

Floyd and McGrattan [85] developed a more complicated model with the consideration of atom nitrogen and *M* (which is not C, H, O, or N). This is a two-steps reaction, detailed equations were developed with a consideration of all the species:

$$\begin{cases} \text{Step 1}: C_xH_yO_zN_aM_b + \upsilon_{O_2}O_2 \rightarrow \upsilon_{H_2O}H_2O + (\upsilon''_{CO} + \upsilon_{CO})CO + \upsilon_{soot}Soot + \upsilon_{N_2}N_2 + \upsilon_M M \\ \text{Step 2}: \upsilon''_{CO}(CO + \tfrac{1}{2}O_2 \rightarrow CO_2) \end{cases} \tag{22}$$

where *M* is a species representing portion of the fuel that is not C, H, O or N. Note that CO has two stoichiometric coefficient where υ''_{CO} applies to the CO that can be converted to CO_2 and υ_{CO} applies to the CO that exists post-flame, and oxidation rate of CO can be seen in [86]; and υ_{H_2O}, υ_{soot}, υ_{N_2}, and υ_M are stoichiometric coefficient of water, soot, nitrogen and species *M*, respectively.

These stoichiometric coefficients are obtained by gas yields and mass fraction:

$$\begin{aligned} &\upsilon_{N_2} = \frac{a}{2}, \quad \upsilon_{H_2O} = \frac{y}{2} - Y_H\upsilon_{soot}, \\ &\upsilon'_{O_2} = \frac{\upsilon'_{CO} + \upsilon_{H_2O} - z}{2}, \quad \upsilon'_{CO} = x - \upsilon_{CO} - (1-Y_H)\upsilon_{soot}, \\ &\upsilon_{O_2} = \upsilon_{CO_2} + \frac{\upsilon_{H_2O} - z}{2}, \quad \upsilon_{CO} = \frac{M_s}{M_{CO}}y_{CO}, \\ &\upsilon_{CO_2} = x - (1-Y_H)\upsilon_{soot}, \quad \upsilon_{soot} = \frac{M_s}{M_{soot}}y_{soot}, \\ &\upsilon_M = b, \quad M_{soot} = Y_H M_H + (1-Y_H)M_C \end{aligned} \tag{23}$$

where Y_H is the atom fraction of hydrogen in the soot; y_{CO} and y_{soot} are the user-specified post-flame yields of CO and soot; *x*, *y*, *z*, *a* and *b* are coefficients which come from the specification of the fuel molecule; and *M* is molecular weight, kg/mol.

2.2.4. Combustion of volatiles

The combustion of most fuels mainly starts at the reaction of volatiles [87]. Combustion and reforming of volatile species may have a great impact on the outlet gas composition, carbon conversion and gasification efficiency [88]. Mainly, up to half of the coal specific energy comes from its volatile contents. Coal volatiles combustion, set free during a gasification process, have a noticeable impact on char combustion reaction rate, outlet gas composition, heat and mass transfer inside the bed as well as the freeboard, and mixing patterns [89].

Experimental observations on combustion of pre-mixed gases in fluidized beds identified three combustion regimes [90]: (1) at low bed temperatures (less than about 970–1020 K), the volatiles may not burn within the bed; (2) at moderate bed temperatures (from about 1100–1170 K), the volatiles are likely to burn only in the bubbles; and (3) at high bed temperatures (greater than about 1170 K), combustion may occur within the bubbles and in the particulate phase of the bed. Many research focused on the modeling of gas combustion in fluidized bed, and a summary of these mathematical models can be seen in Refs. [88,90,91].

One could imagine that the kinetics of the homogeneous combustion and reforming reactions are well know, but this is not the case. The reaction between the stable chemical species involved in the homogeneous reaction are a complex combination of several elementary reaction [88]. However, it is commonly assumed that volatiles burn via the steps [67]:

$$\begin{cases} Volatiles + O_2 \rightarrow CO + H_2O \\ CO + 0.5O_2 \rightarrow CO_2 \end{cases} \tag{24}$$

There is a great amount of work on the kinetics of these homogeneous reactions. Some authors have analyzed the difference in the kinetics available in the literature, especially for the homogeneous oxidation of CO [88–92].

It would be improper to remove volatile effects when developing a model for combustion of solid particles. A particle combustion model considering volatile effects was established by Li and You [87] to provide solution to simulate combustion process of different kinds of particles. The results demonstrated that this model has adequate accuracy and quite a shorter calculation time. Eslami et al. [89] also employed a sequential model for coal volatile combustion to predict the behavior of corresponding fluidized bed reactors in coal gasification processes. It was shown that the model can successfully predict coal's volatile matter combustion behavior

without any further need for solving coupled nonlinear differential equations in an equation-oriented manner.

Turbulent non-premixed coal flames generated from volatiles combustion undergo significant departures from chemical equilibrium through super-equilibrium radical concentrations, extinction and sooting and some aspects of pollutant formation. One possible route to include all these effects in turbulent flow calculations is the laminar flamelet model [67,93,94]. In the flamelet model [95] for the gas-phase volatile combustion of coal, local temperature and major species concentrations were given by the mixture fraction. This approach provided a way of incorporating finite rate chemistry effects in turbulent coal volatile combustion modeling. It was assumed that radius of curvature of the flame front is much larger than its thickness and this allowed the analysis of flamelet flow-field to be approximated by the boundary layer assumption. Thus, the series of governing equations can be reduced into one-dimensional form to solve for the temperature and concentrations as a function of a single independent variable.

2.3. Physical process

2.3.1. Transportation of gas volatiles

Production of individual gas volatiles, such as CO, CO_2 and H_2O, were frequently ignored in the modeling. Kung [8] developed a model considering a mixture of all gas volatiles, which was gained by mass loss. Gas volatiles were regarded as flowing out the wood slab immediately after their generation. Transportation of gas volatiles inside the woods slab was ignored. Later, some models used Darcy's law to describe the gas transportation inside combustible materials [96–100].

Neglecting contribution of the inert initially present in the pores of the solid, the velocity and pressure of gas volatiles can be given by Darcy's law and the ideal gas law respectively [101]:

$$u = -\frac{\gamma}{\mu}\frac{\partial P}{\partial x} \tag{25}$$

$$P = \frac{\rho_g RT}{M_g} \tag{26}$$

Mean molecular weight of vapor/gas phase mixture can be given as:

$$\frac{1}{M_g} = \sum_i \left(\frac{Y_i}{M_i}\right) \tag{27}$$

where Y_i is the mass fraction of species i; M_i is the molecular weight of species i, kg/mol.

Henderson and Wiecek [102] considered a porous material to calculate the mass flux of gas volatiles. The mass flux of gases, $\dot{m}''_g$, was calculated using Darcy's law in the following form:

$$\dot{m}''_g = -\frac{\gamma m_g}{\mu_g \phi \Delta x \Delta A}\frac{\partial P}{\partial x} \tag{28}$$

And the pressure was calculated by the equation of state, that is:

$$P = \frac{m_g RT}{M_g \phi \Delta x \Delta A} \tag{29}$$

Above equations described gas transportation inside solid phase. Two properties were used in these equations, such as permeability and porosity. These two properties are temperature dependent, which will be introduced in the following sections.

2.3.2. Thermal shrinkage

Although many models [10,24,25,101,103–117] have described volume shrinkage, no common agreement was addressed. Several approaches used to describe volume shrinkage are concluded:

- The most frequently used approach is connected with other properties, such as pore volume, mass conversion, etc. Di Blasi [101] assumed that volume occupied by solid decrease linearly with the wood mass and increase with the char mass by a shrinkage factor. Shi and Chew [80,81] also considered that wood shrinkage is connected with mass loss. Larfeldt et al. [106] described shrinkakge of solid by including a relationship in conservation equation. Shrinkage was envisaged to occur with reduction or expansion of pore volume by Hastaoglu and Berruti [103]. Volume of each cell at any time can be then evaluated. Bellais et al. [112] used radial and longitudinal shrinkage coefficients to describe shrinkage of woods, which were calculated through interpolation by assuming that particle shrinks linearly with an averaged conversion. Yang et al. [115] described shrinkage by mass loss of solid to gas phase.
- The second approach is the data obtained by experiments. Hastaoglu and Hassam [105] recorded a set of shrinkage data as a function of time (conversion) and used them in the modeling. Hagge and Bryden [108] used experimentally available data for shrinkage factor in modeling.
- The third approach described relationship between shrinkage and external heat flux. Bryden et al. [110] used a shrinkage factor dependent on external heat flux to describe shrinkage of woods.
- The last one is the shrinking velocity. Lede [104] assumed a shrinking velocity profile to describe the shrinkage of woods.

Shrinkage occurs in the char layers during the pyrolysis reactions because of a rearrangement of chemical bounds and the coalescence of graphite nuclei within the biomass particle [108]. Shrinkage factor is defined as [118]:

$$f = \frac{L_c - L_{res}}{L_0 - L_{res}} \tag{30}$$

where L_c is the thickness of the charred sample, m; L_{res} is the thickness of the residue after the char was removed, m; and L_0 is the original thickness, m.

Tran and White [118] investigated shrinkage of woods under a heat flux range between 15 and 55 kW/m^2, shown in Table 6. Results showed that shrinkage factor increases with a higher heat flux.

For polymers, it is difficult to find these kind of experimental data. This may be because that polymers melt at high temperature and go through irregular shrinkage or expansion.

2.3.3. Permeability

Air permeability of a porous material characterizes the capacitance of this material to let such a fluid permeate under a total pressure gradient [119]. Permeability is defined by Darcy's equation, which is expressed as [120]:

$$\gamma = \frac{\dot{m}''_{H_2O,vol} \cdot \mu \cdot L}{\Delta A \cdot \Delta P} \tag{31}$$

where $\dot{m}''_{H_2O,vol}$ is the volumetric flow rate of water of viscosity μ through a cross-sectional area ΔA and length L of cell water under an applied osmotic pressure difference ΔP.

Three approaches were found in previous models to obtain temperature-dependent permeability. The first approach is an empirical model. Henderson and Wiecek [23] developed a model to describe permeability by mass loss and temperature, which was expressed as:

$$\frac{1}{\gamma_0}\frac{\partial \gamma}{\partial t} = \Psi_v F \frac{\partial T}{\partial t} + \Psi_c (1-F)\frac{\partial T}{\partial t} + \frac{\zeta}{m_0}\frac{\partial m}{\partial t} \tag{32}$$

where F is the instantaneous mass fraction, which can be obtained by $(m - m_f)/(m_v - m_f)$; Ψ_v and Ψ_c; is coefficient of linear

Table 6
Measured wood properties related to charring.

Species	Flux (kW/m^2)	Shrinkage factor, f	Char yield, y_c	Apparent, ρ_c (kg/m^3)
Redwood (Softwood, 312 kg/m^3)	17.8	0.523	0.27	181
	17.7	0.512	0.27	174
	25.8	0.563	0.26	168
	26.2	–	–	–
	38.5	0.613	0.27	183
	38.7	0.634	0.28	180
	53.6	0.835	0.32	156
	56.3	0.747	0.31	191
Southern pine (Softwood, 508 kg/m^3)	17.4	0.475	0.20	272
	17.4	0.456	0.24	287
	25.2	0.530	0.30	287
	26.9	0.469	0.20	294
	38.5	0.479	0.25	358
	38.6	0.444	0.23	355
	55.5	0.616	0.25	256
	56.0	0.583	0.26	312
Red oak (Hardwood, 660 kg/m^3)	17.8	0.547	0.25	327
	18.7	0.567	0.26	328
	25.0	0.559	0.24	317
	25.8	0.564	0.25	333
	37.8	0.625	0.25	360
	38.4	0.606	0.25	345
	53.1	0.753	0.27	256
	53.6	0.705	0.31	312
Basswood (Hardwood, 420 kg/m^3)	17.6	0.428	0.24	264
	17.8	0.408	0.22	251
	27.7	0.421	0.23	288
	25.5	0.430	0.22	260
	38.1	0.450	0.23	255
	38.7	0.409	0.20	227
	51.6	0.519	–	–
	53.4	0.523	0.23	239

Table 7
Average permeability of four kinds of woods.

Woods	Position	Permeable direction	Average permeability (m^2)
Pinus koralensis	Sapwood	Axial	8.66×10^{-9}
		Tangential	7.60×10^{-13}
		Radial	1.15×10^{-12}
	Heartwood	Axial	1.83×10^{-9}
		Tangential	3.83×10^{-14}
		Radial	2.87×10^{-13}
Larix dahurica	Heartwood	Axial	1.26×10^{-9}
		Tangential	5.21×10^{-14}
		Radial	6.80×10^{-14}
Populus davidiana	Sapwood	Tangential	0.83×10^{-10}
		Radial	5.31×10^{-13}
	Heartwood	Axial	2.98×10^{-8}
		Tangential	1.08×10^{-13}
		Radial	7.81×10^{-14}
Betula platyphylla	Sapwood	Tangential	4.94×10^{-9}
		Radial	2.46×10^{-12}
	Heartwood	Tangential	4.02×10^{-12}
		Radial	2.30×10^{-12}

permeability of virgin material and char, respectively, 1/K; and ζ is decomposition permeability coefficient.

Another approach is interpolation between virgin materials and char. Some part of virgin material change into char when pyrolysis reaction is taking place. Permeability of the whole solid phase changes when more char is producing. The whole permeability may be dependent on percentages of virgin material and char. Permeability was then assumed to vary with composition of solid species by Hagge and Bryden [108]:

$$\gamma = \eta\gamma_v + (1-\eta)\gamma_c \tag{33}$$

where η is a reaction progress variable,

$$\eta = \frac{m}{m_{v,0}} \tag{34}$$

Wood permeability was a physical property of anisotropy in different grain directions. Wang et al. [121] measured average permeability of four species of common woods, and the results are shown in Table 7. Unfortunately, these data are only the average permeability of woods under room temperature.

For the third approach, some researchers used permeability coefficient to describe polymers' ability of transporting gases.

Table 8
Permeability coefficients and activation energy of permeation of polymers.

Polymer	Permeant	Temp. (°C)	Pe × 10^{13}	Temp. range (°C)	Pe_0 × 10^7	E_p (kJ/mol)
LDPE	O_2	25	2.2	5–60	66.5	42.7
	CO_2	25	9.5	5–60	62.0	38.9
	CO	25	1.1	5–60	154	46.5
	N_2	25	0.73	5–60	329	49.4
	H_2O	25	68	10–90	48.4	33.5
HDPE	O_2	25	0.30	5–60	0.423	35.1
	CO_2	25	0.27	5–60	0.0506	30.1
	CO	25	0.15	5–60	1.15	39.3
	N_2	25	0.11	5–60	0.991	39.7
	H_2O	25	9.0	–	–	–
PP	N_2	30	0.33	20–70	1280	55.7
	O_2	30	1.7	20–70	278	47.7
	CO_2	30	6.9	20–70	24.0	38.1
	H_2O	30	51.0	10–90	900	42.3
PS	O_2	25	2.0	–	–	–
	N_2	25	0.59	–	–	–
	CO_2	25	7.9	–	–	–
	H_2O	25	840	–	–	–
PMMA	O_2	34	0.116	–	–	–
	H_2O	23	480	–	–	–
PVC	N_2	25	0.0089	25–80	9380	69.0
	O_2	25	0.034	25–80	179	55.8
	CO_2	25	0.12	25–90	930	56.8
	H_2O	25	206	25–80	2.04	22.9

Permeability coefficient is not only a function of the chemical structure of the polymer, it also varies with the morphology of the polymer and depends on many physical factors such as density, crystallinity, and orientation [122]. The permeability coefficient can be expressed by:

$$Pe = \frac{m_g L}{t \Delta A \Delta P} \tag{35}$$

where Pe is the permeability coefficient, cm^3 (273.15 K; 1.013×10^5 Pa) cm/cm^2 s Pa.

Permeability coefficient of polymer is dependent on temperature, which can be represented by:

$$Pe = Pe_0 \cdot \exp\left(-\frac{E_p}{RT}\right) \tag{36}$$

where Pe_0 is the pre-exponential factor, cm^3 (273.15 K; 1.013×10^5 Pa) cm/cm^2 s Pa; E_p is the activation energy of permeation, kJ/mol;

Table 8 shows a summary of permeability coefficient of polymers [122]. Usage of these data in describing fire processes may be limited because of small applicable temperature ranges.

Among above approaches, empirical model may be the best one to gain temperature dependent permeability. However, the above empirical model seems to be a little complicated as there are too many input variables which are needed to be gained from experiments. It is expected that a simpler empirical model can be developed in future work. The approach of interpolation may be limited as the permeability may not be accurately followed by percentages of virgin material and char. And applications of permeability coefficients for polymers may be restricted in describing fire processes because of small applicable temperature ranges.

2.3.4. Water evaporation

Our previous studies showed that water has influence on several fire behaviors, such as ignition time [123,124], CO production [77], etc. There are two kinds of water in woods: bond water and free water. Fiber saturation point has been defined as the moisture content at which cell walls are saturated with bound water with no free water in the lumens [125]. The fiber saturation point was given by [126]:

$$X_{sat} = Max(X^0_{sat} + 0.298 - 0.001T, 0.2) \tag{37}$$

where X^0_{sat} is the moisture content at fiber saturation point at ambient temperature, which is about 0.3 for most wood species; and T is temperature in °C.

Water absorption at saturation of polymers is much smaller than that woods. Table 9 shows a summary of water absorption at saturation of polymers [127]. Some polymer showed a range of data in this table as they were obtained from different sources. It is noticed that most of the data is less than 0.01. Water absorption at saturation of some polymers are much higher, such as PA 6, PA 66, PBT. Starzhenetskaya and Davydova [128] established quantitative parameters of reversibility of the sorption–desorption process and diversity of the states of water sorbed. Results showed that water in the polymers was in free and loosely bound states. So the water inside polymers may be considered as free water.

Water evaporation of materials can be expressed by Arrhenius equation. This can be treated as a heterogeneous reaction [129]:

$$\frac{\partial c_{evap}}{\partial t} = -A \cdot \exp\left(-\frac{E}{RT}\right) c_{H_2O} \tag{38}$$

Table 9
A summary of water absorption at saturation of polymers.

Materials	Water absorption at saturation
PMMA	0.003–0.022
PE	0.001
PS	0–0.042
ABS	0.003–0.01
PC	0.0015–0.0037
PVC	0.004
PET	0.004–0.005
PBT	0.0008–0.078
PA 6	0.05–0.10
PA 66	0.07–0.09
PP	0.0001

Bryden et al. [110] considered 95 °C as evaporation start temperature. It was suggested that evaporation process happens when temperature is higher than 95 °C. This model also used an Arrhenius type expression, which was given as:

$$Moisture \overset{k_{evap}}{\rightarrow} water\ vapor \tag{39}$$

where

$$\begin{cases} \dot{m}''_{H_2O} = 0, & T < 95\ ^\circ C \\ \dot{m}''_{H_2O} = k\rho_m, & T > 95\ ^\circ C \end{cases} \tag{40}$$

where ρ_m is the density of mixture, kg/m^3. It was suggested that kinetic parameters of $A = 5.13 \times 10^6$ s^{-1} and $E = 88$ kJ/mol.

Sand et al. [126] calculated the rate of water evaporation in solid materials as:

$$\dot{m}''_{H_2O} = k \cdot \rho = \frac{C_{p,H_2O}(T - T_{sat})}{\Delta h_{evap}\Delta t} \cdot \rho \tag{41}$$

where T_{sat} is temperature at fiber saturation point, typically 373.15 K, however this is only true for free boiling water and the physical structure of the wood will induce an increase of the saturation temperature.

In Eq. (41), Δh_{evap} is influenced by whether material has achieved fiber saturation point or not. Heat of evaporation of free liquid water and heat of desorption were respectively given as follows [126]:

$$\Delta h_l = 3.179 \times 10^6 - 2.5 \times 10^3 (T - 273.15) \tag{42}$$

$$\Delta h_{desorp} = 1.176 \times 10^6 \exp(-15.0 X_{bound}) \tag{43}$$

If moisture content is higher than that at fiber saturation point, only the free water vaporizes. Otherwise, energy consumed must contain the energy of changing bound water into free water, and energy for vaporizing this free water. So it is considered that the evaporative heat of water considering fiber saturation point as a turning point [126]:

$$\begin{cases} \Delta h_{evap} = \Delta h_l, & X \geqslant X_{sat} \\ \Delta h_{evap} = \Delta h_l + \Delta h_{desorp}, & X < X_{sat} \end{cases} \tag{44}$$

The rate of water evaporation under different moisture content can be given by:

$$\begin{cases} k_{evap} = \frac{C_{p,H_2O}(T - T_{sat,l})}{(\Delta h_l)\Delta t}, & X \geqslant X_{sat} \\ k_{evap} = \frac{C_{p,H_2O}(T - T_{sat,bound})}{(\Delta h_l + \Delta h_{desorp})\Delta t}, & X < X_{sat} \end{cases} \tag{45}$$

Above models have described water evaporation of free water and bound water inside woods. And evaporative heat of water can be calculated when moisture content is higher or less than fiber saturation point. Starzhenetskaya and Davydova [128] found that the water in polymers can be assumed as free water by experiments. So water evaporation process of polymers is similar to the woods with free water. Arrhenius equation can describe water evaporation inside woods and polymers well.

2.3.5. Thermal expansion

Although a large number of models [23,130–146] have considered thermal expansion, no common agreement was found. Several approaches were used to describe thermal expansion of polymers:

- The first approach is connected with other properties. Stagges [131] determined net volume change by production rate of gas volatiles within the slice and difference between inflow and outflow rates of gas volatiles. Feih et al. [133,134,136] considered thermal expansion as a function of temperature based on experimental results. Anderson and Wauters [137] simulated the pyrolysis and combustion processes of coating by assuming expansion as a function of mass loss. Henderson et al. [23,139] expressed expansion by using a modified Lagrangian control system, in which the control volume was a function of temperature and time.
- The second approach is coefficient. Sullivan and Salamon [130] used a defined coefficient to describe expansion. This coefficient is also used to calculate thermal strains and stress.
- The last approach is empirical model. Di Blasi [145] introduced an empirical parameter of expansion factor but limit the maximum volume expansion.

Table 10
The coefficient of linear thermal expansion.

Name	Density (kg/m^3)	Coefficient of linear thermal expansion (1/K)
PMMA	1180	7.2×10^{-5}
PS	1040	5.7×10^{-5}
HDPE	967	2.31×10^{-4}
LDPE	920	2.70×10^{-4}
PTFE	2189	1.27×10^{-4} (25–60 °C)
Cellulose	–	7.5×10^{-5} (25–50 °C)
	–	5.2×10^{-5} (−10 to 25 °C)

Thermal expansion is a tendency of matter to change in volume in response to a change in temperature. Rate of length change of the solid materials was calculated by Henderson and Wiecek [102]:

$$\frac{1}{L_0}\frac{\partial L}{\partial t} = \beta_w F \frac{\partial T}{\partial t} + \beta_c (1 - F)\frac{\partial T}{\partial t} + \frac{\eta}{m_0}\frac{\partial m}{\partial t} \tag{46}$$

where β_v and β_c is the coefficient of linear expansion of virgin material and char, respectively, 1/K; F is the instantaneous mass fraction, which can be obtained by $(m - m_f)/(m_v - m_f)$; and η is the decomposition expansion factor.

The first and second terms on the right-hand side of Eq. (46) represent the thermal expansion/contraction of the virgin and char components, respectively. Each term is weighted by instantaneous mass fraction. Expansion due to pyrolysis of the solid material is given by the last term on the right.

Klason et al. [147] assumed a linear dependence of thickness on the temperature, which was expressed by:

$$\frac{\partial L}{\partial T} = \beta \cdot L \tag{47}$$

where β is the coefficient of thermal expansion, which can be obtained by experiments, shown in Table 10.

Murthy and Rani Rao [148] investigated linear thermal expansion coefficient (β) in a temperature range of 20–200 °C by using a two-terminal capacitance technique. Linear thermal expansion

Table 11
Linear thermal expansion coefficient of polymers dependent on temperature.

Temperature (K)	Polyester ($\beta \times 10^5$)	PE ($\beta \times 10^5$)	PTFE ($\beta \times 10^5$)
313	9.2	7.0	-
323	10.0	7.0	4.7
333	10.0	13.3	4.7
343	10.0	13.3	4.7
353	10.4	14.9	4.7
363	10.9	15.9	4.7
373	14.9	21.0	10.2
383	16.2	37.1	12.3
393	19.8	78.6	13.6
403	24.7	78.2	33.3
413	39.3	144.9	45.7
423	65.2	395.5	53.9
433	77.5	814.0	67.0

coefficients of polymers at different temperature are shown in Table 11.

To describe thermal expansion, Henderson and Wiecek's model [102] is a complicated one as there are many input variables which are needed to be gained from experiments. Models by Klason et al. [147] and Murthy and Rani Rao [148] are simpler. Measurement of temperature dependent linear thermal expansion coefficient were taken by Murthy and Rani Rao [148]. However, the measurements only focused on three polymers, and more experiments on other polymers are expected in future work.

2.3.6. Porosity

Porosity is a fraction of the volume of voids over the total volume, which is between 0 and 1. The porosity of woods can be estimated by [149]:

$$\phi = 1 - \frac{\rho_{ave}}{\rho_{theor}} \tag{48}$$

where ρ_{ave} is average apparent density of the woods; and ρ_{theor} is a theoretical density of compact solid wood free from voids, which is usually assumed to be 1500 kg/m^3.

De Souza Costa and Sandberg [150] also considered that woods' porosity was moisture dependent, and the porosity of wood and char were estimated by:

$$\phi_v = 1 - \frac{\rho_v}{1500 - 1.35\rho_v X}, \quad X < 0.3 \tag{49}$$

$$\phi_c = 1 - \frac{\rho_c}{\rho_C} \tag{50}$$

where ρ_C is the density of carbon, which is usually assumed to be 1957 kg/m^3. These two equations indicate that low-density wood has a higher porosity than high-density wood, and lower moisture content wood has a higher porosity.

No empirical model has been found to calculate porosity of polymer by density. Henderson and Wiecek [23] used interpolated values between char and virgin polymer to describe the whole porosity. Moreover, Florio et al. [139] assumed that porosity of polymers was dependent on mass loss, which was expressed by:

$$\frac{1}{\phi_0}\frac{\partial \phi}{\partial t} = \frac{\delta}{m_0}\frac{\partial m}{\partial t} \tag{51}$$

where δ is decomposition porosity coefficient.

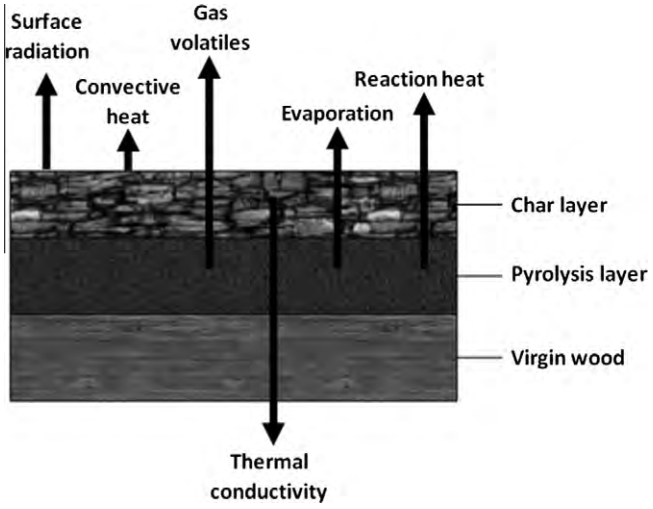

Fig. 4. Fire processes of woods under external heat flux.

From above models, it is noticed that porosity of woods can be simply described by their densities. However, few models have been found to describe the porosity of polymers.

2.3.7. Tension and compression

Although previous models [20,133,134,136,151–153] have investigated tension and compression of materials under both heating and loading, applications are still limited as the investigations only focused on composites. Few one-dimensional models have been used to simulate mechanical behaviors of pure polymers and woods.

Mouritz and Mathys [154] formulated a two-layer model based on rule-of-mixtures to predict the residual tension of polymer laminates following fire. Later, this model was used to predict the time-to-failure of laminate subjected to combined tension loading and one-side heating by Feih et al. [152]. This model assumed that laminate can be treated as a two-layer material: char layer nearest to heated surface and virgin layer on the other side. Tension through two layers was assumed as constant, which was expressed by:

$$\sigma = \left(\frac{L_0 - L_c}{L_0}\right)\sigma_0 + \left(\frac{L_c}{L_0}\right)\sigma_c \tag{52}$$

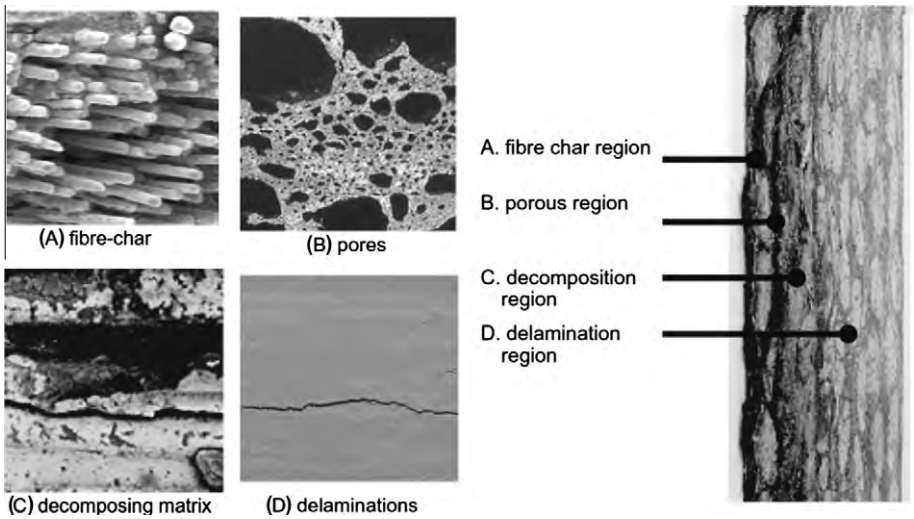

Fig. 3. Cross-sectional view of the fire-damaged laminate.

Table 12
A summary of considerations in previous one-dimensional models for woods.

Models	Year	Material	Heat conduction	Pyrolysis	Gas volatiles	Volume change	Internal gas pressure	Water evaporation	Permeability	Porosity	Mechanical behaviors
Hadvig and Paulsen [158]	1965	Wood	•	•	•						
Tinney [7]	1965	Wood	•	•	•						
Panton and Rittmann [159]	1971	Organic solid	•	•	•						
Kung [8]	1972	Wood	•	•	•						
Kansa et al. [28]	1977	Wood	•	•	•		•		•	•	
White and Schaffer [26]	1978	Wood	•	•	•						
Chan et al. [42]	1985	Biomass	•	•	•		•	•	•	•	
Parker [25]	1986	Wood	•	•	•	•		•			
Sibulkin [160]	1986	Charring material	•	•	•						
Capart et al. [161]	1988	Wood	•	•	•						
Alves and Figueiredo [24]	1989	Wood	•	•	•	•	•	•	•		
Hastaoglu et al. [103]	1989	Wood	•	•	•	•	•			•	
Koufopanos et al. [162]	1991	Biomass	•	•	•						
Aerts and Ragland [10]	1990	Wood	•	•	•	•	•	•		•	
Fredlund [163]	1993	Wood	•	•	•		•	•	•		
Shrestha et al. [164]	1994	Wood	•	•				•			
Wagenaar et al. [165]	1994	Biomass	•	•	•		•				
Lede [104]	1994	Biomass	•	•	•	•				•	
Di Blasi [13,166]	1994	Cellulose	•	•	•		•		•	•	
Hastaoglu and Hassam [105]	1994	Wood	•	•	•	•	•			•	
Saastamoinen et al. [167]	1996	Biomass	•	•	•			•		•	
Ahuja et al. [168]	1996	Wood	•	•	•						
Di Blasi [101]	1996	Biomass	•	•	•	•	•		•	•	
Bilbao et al. [169]	1996	Wood	•	•	•			•			
Moghtaderi et al. [15]	1997	Wood	•	•	•						
Mogheaderi et al. [170]	1998	Wood	•	•	•		•	•		•	
Jia et al. [171]	1999	Charring material	•	•	•						
Larfeldt et al. [106]	2000	Wood	•	•	•	•	•		•	•	
Janse et al. [172]	2000	Wood	•	•	•		•			•	
Gronli and Melaaen [173]	2000	Wood	•	•	•		•	•	•	•	
Spearpoint and Quintiere [174]	2000	Wood	•	•	•		•	•			
Peters and Bruch [129,175]	2001	Wood	•	•	•			•		•	
Mousques et al. [176]	2001	Wood	•	•	•		•		•	•	
Di Blasi [107]	2002	Wood	•	•	•	•			•	•	
Hagge and Bryden [108]	2002	Biomass	•	•	•	•	•	•	•	•	
Klose and Schinkel [109]	2002	Wood	•	•		•				•	
Bryden et al. [110]	2002	Wood	•	•	•	•	•	•	•	•	
Bruch et al. [111]	2003	Wood	•	•	•	•	•	•	•	•	
Babu and Chaurasia [17,177–179]	2003	Wood	•	•	•		•		•	•	
Bellais et al. [112,180]	2003	Wood	•	•	•	•				•	
Janssens [181]	2004	Wood	•	•	•	•		•			•
Galgano and Di Blasi [113]	2004	Wood	•	•	•	•		•			
Theuns et al. [114,182]	2005	Charring material	•	•	•	•					
Shen et al. [183]	2007	Wood	•	•	•			•			
Yang et al. [115]	2007	Waste	•	•	•	•	•	•		•	
Vijeu et al. [99]	2008	Wood	•	•	•		•	•	•	•	
Sadhukhan et al. [116,184]	2008	Biomass	•	•	•	•			•		
Craft et al. [185]	2008	Wood frame	•	•	•		•	•	•	•	
Larfeldt et al. [117]	2008	Wood	•	•	•	•	•	•	•	•	
Ratte et al. [97]	2009	Wood	•	•	•		•	•	•	•	
Lautenberger and Fernandez-pello [98]	2009	Wood	•	•	•		•	•	•	•	
Grieco and Baldi [186]	2011	Wood	•	•	•		•	•			
Dufour et al. [187]	2011	Biomass	•	•	•		•		•		
He and Behrendt [76]	2011	Biomass	•	•	•	•	•	•			
Shi and Chew [80,81]	2012	Wood	•	•	•	•		•		•	

where σ_c is the tension of char, which is assume to be negligible based on experimental strength measurements.

Many models [20,130,133,134,136,151–153] have described compression of combustible materials under external heat flux and loading. A semi-empirical model describing relationship between compression and temperature was developed by Gibson et al. [133,151]:

$$\sigma(T) = \left[\frac{\sigma_0 + \sigma_f}{2} - \frac{\sigma_0 + \sigma_f}{2}\tan h(\Phi(T - T_f))\right]R(T)^n \quad (53)$$

where Φ is a material constant describing temperature range over which compression is reduced during thermal softening process; σ_0 is the strength remaining at the room temperature value until the laminate is heated to critical softening temperature, which can be calculated using laminate theory or measured; σ_f, T_f, and Φ must be fitted to an elevated temperature compression test data of the laminate; $R(T)$ is a scaling function to account for mass loss due to pyrolysis of the polymer matrix; and the exponent n is an empirical value. When $n = 0$ it is assumed that the decomposition has no effect on the compressive strength. And when $n = 1$ it is

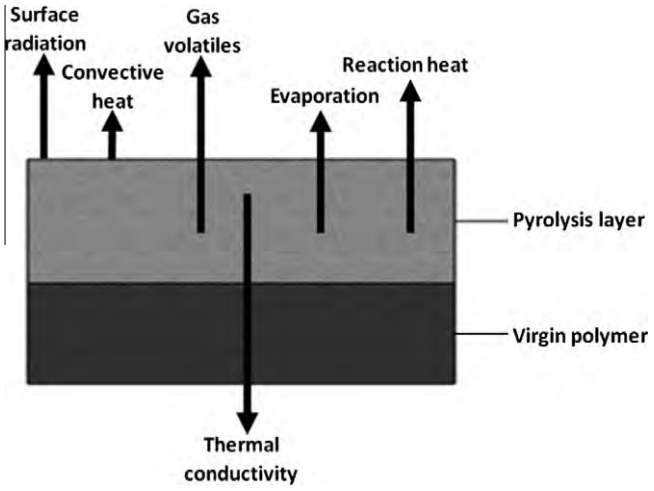

Fig. 5. Fire processes of non-charring polymers under external heat flux.

assumed that a linear relationship exists between mass loss and strength loss.

After temperature profile through a laminate has been calculated using thermal equation, residual compression is calculated at a number of locations in the through-thickness direction using Eq. (53). The bulk compression is then determined by integrating these values over the thickness of the laminate using the Simpson integration technique with m intervals, where m must be an even number [133]. And the compression can be given as [133,151]:

$$\int_0^L \sigma(x)dx = \frac{L}{3m}[\sigma(x_0) + 4\sigma(x_1) + 2\sigma(x_2) + \ldots + 2\sigma(x_{n-2}) + 4\sigma(x_{n-1}) + \sigma(x_n)] \quad (54)$$

$$\sigma_{ave} = \frac{1}{L}\int_0^L \sigma(x)dx \quad (55)$$

Compressive failure is assumed to occur once average compression is reduced to the compressive stress applied to the laminate. The time taken for the strength to reach the applied compression is taken to be the time-to-failure.

Temperature-dependent Young's modulus was used to calculate tension or compression of materials under heating and loading, which was given by [19,134]:

$$E(T) = E_0\left(1 - \frac{T - T_0}{T_f - T_0}\right)^m \quad (56)$$

where E_0 is the modulus at ambient temperature; T_f is the elevated temperature at which the Young's modulus vanishes. The power law index m can be taken between 0 and 1. The extreme case $m = 0$ represents no degradation, and $m = 1$ linear degradation with temperature.

2.4. Failure process

Serious concern was raised about failure of combustible materials under both heating and loading in recent years. Fire-included damage experienced by laminates includes matrix decomposition, pore formation, delamination cracking, matrix cracking, fiber–matrix debounding, and char formation, shown in Fig. 3 [6]. Modeling is the simplest and low-cost way for the prediction of structure failure [11,133,152,155].

Experiments by Elmughrabi et al. [156] showed that fire reaction properties, heat release rate and smoke production, and time-to-ignition were affected by external loading. So modeling of combustible materials may be different when combustible materials are positioned under both heating and loading. An integrated model which can describe fire processes of combustible materials under external heat flux and loading is critically needed.

Fire-induced damage to composite structures is difficult to simulated accurately because it is dependent on many parameters, with the main factors being the temperature and duration of the fire; the volumetric dilations and toughness properties of the material at high temperature; and the type and magnitude of external loading (including the boundary conditions) [6]. And absence of experimental data or empirical model in these aspects hampers modeling accuracy of failure process.

3. Typical models for combustible materials

3.1. Woods

Woods are the most frequently used combustible materials in one-dimensional modeling. They can be classified into hardwoods and softwoods, which have different percentages of cellulose, hemicelluloses and lignin. These three components have quite different thermal pyrolysis characteristics. Experiments showed that these components decompose to release volatiles over different temperature ranges [1]. Cellulose is from 240 to 350 °C, hemicelluloses is from 200 to 260 °C, and lignin is from 280 to 500 °C.

Solid phase of woods under external heat flux can be divided into three layers. The upper, middle and bottom layers are char layer, pyrolysis layer and virgin wood, respectively. Char front is

Table 13
A summary of considerations in previous one-dimensional models for non-charring polymers.

Models	Year	Material	Heat conduction	Pyrolysis	Gas volatiles	Volume change	Internal gas pressure	Water evaporation	Permeability	Porosity	Mechanical behaviors
Di Blasi et al. [188,189]	1991	PMMA	•	•	•		•				
Quintiere and Iqbal [190]	1994	PMMA	•	•	•						
Di Blasi [191]	1996	PMMA	•	•	•						
Moghtaderi et al. [15]	1997	PMMA	•	•	•						
Staggs [192,193]	1999	PMMA, PE	•	•	•	•					
Di Blasi [2]	1999	PE	•	•	•					•	
Bourbigot et al. [141]	1999	PP	•	•	•	•	•		•	•	
Zhou and Fernandez-Pello [143]	2000	PP	•	•	•	•					
Zhou et al. [194]	2002	PMMA	•	•	•						
Esfahani and Kashani [195]	2006	PMMA	•	•	•		•				
Rein and Bal [196,197]	2008	PMMA	•	•	•						
Stoliarov et al. [48]	2009	PMMA, HIPS, HDPE	•	•	•	•	•	•		•	
Lautenberger and Fernandez-Pello [21,135]	2009	PMMA	•	•	•	•	•	•	•	•	
Chaos et al. [198]	2011	PMMA	•	•	•	•					

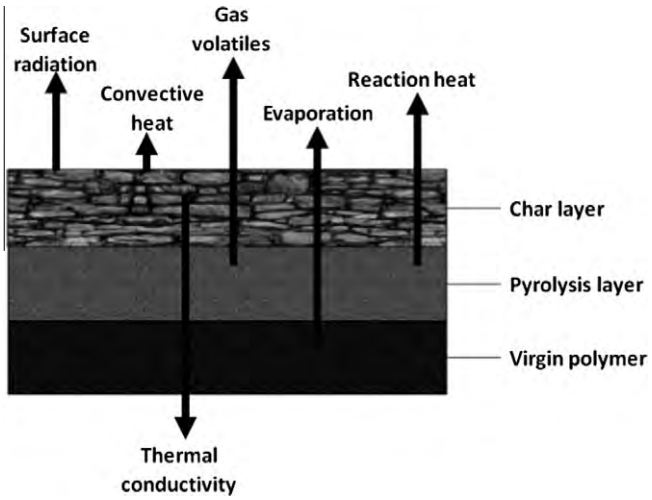

Fig. 6. Fire processes of charring polymers under external heat flux.

defined as the transition between the char layer, a zone of cracked charcoal that has no relevant strength or stiffness properties, and the pyrolysis layer, the zone where thermal degradation of wood and char formation are actually occurring. This transition is usually considered to be located at the 300 °C isotherm, named the char-line [157].

When external heat flux affects the woods' surface, parts of heat are reflected to the air by radiation. This radiation heat is dependent on surface emissivity of woods, and surface and ambient temperatures. Part of heat goes straight into wood slab which can be expressed by thermal conductivity. There also exists convective heat between wood's surface and surrounding air. In pyrolysis layer, water evaporation, pyrolysis reactions and production of gas volatiles occur. During water evaporation process, bound water first changes into free water after absorbing heat. The water vapor is then produced by vaporization of free water. Vapor and gas volatiles exhaust through pores, which can be expressed by Darcy's law. Fire processes of woods under external heat flux are shown in Fig. 4.

Table 12 shows a summary of considerations of fire processes in previous one-dimensional models. It is known that almost all of the models have considered heat conduction, pyrolysis reaction and production of gas volatiles. However, modeling of some fire processes, such as shrinkage, internal gas pressure, water evaporation, properties of permeability and porosity, and mechanical behaviors, are less considered in previous models.

3.2. Non-charring polymers

Non-charring polymers burn out with no or very few residue. Their fire processes are similar to the woods, which is shown in Fig. 5. Solid phase of non-charring polymers can be divided into two layers. The upper layer is pyrolysis layer, in which pyrolysis reactions occur. Gas volatiles and vapor are produced in this layer. These gas volatiles exhaust to the air through pyrolysis layer through surface. During this process, mass flux of gas volatiles is determined by several properties, such as permeability, porosity, internal pressure, etc. The bottom layer is virgin polymer. Non-charring polymers burn away completely leaving no or very few residue, which can be modeled using theory similar to flammable liquids [5].

Table 13 shows a summary of considerations in previous one-dimensional modeling for non-charring polymers. It is noticed that consideration of some fire processes, such as internal gas pressure, water evaporation, properties of permeability and porosity, are less taken in previous models. Based on reviewed papers, no model has been found to describe mechanical behaviors of non-charring polymers under both heating and loading.

3.3. Charring polymers

As commonly used in buildings, charring polymers attracted so much attention from researchers and engineers. Fire processes of charring polymers during external heat flux are shown in Fig. 6. Although fire processes are similar to woods, damages will be much serious because of large amount of toxic gas volatiles can be produced. The prediction of toxic gas volatiles are significant as they behave as depending conditions in fire risk evaluation of buildings.

Table 14 shows a summary of considerations in previous one-dimensional models for charring polymers. It is noticed from previous models that most of the investigated polymers are intumescent polymers. In this section, some sandwich panels are considered to be classified into charring polymers as one layers of the sandwich panels are wood or cardboard, even though the other layers are intumescent polymers. Fire processes of these polymer sandwich are much complicated as materials from different layers will be affected by each other.

3.4. Intumescent polymers

When exposed to flame, intumescent polymers undergo several reactions which can be characterized as [146]: (i) melting – polymer matrix melts and degrades to form a viscous fluid. Commercial coatings may also include a fire-retardant component which

Table 14
A summary of considerations in previous one-dimensional models for charring polymers.

Models	Year	Material	Heat conduction	Pyrolysis	Gas volatiles	Volume change	Internal gas pressure	Water evaporation	Permeability	Porosity	Mechanical behaviors
Di Blasi [199]	1997	Waste	•	•	•	•				•	
Krysl et al. [200]	2004	Polymer sandwich	•	•	•						
Gu and Asaro [19,134]	2005	Polymer sandwich	•	•		•					•
Salvador et al. [201]	2008	Cardboard and PE	•	•	•		•	•	•	•	
Lautenberger and Fernandez-Pello [21,135]	2009	Charring material	•	•	•	•	•	•	•	•	
Galgano et al. [96]	2010	Polymer sandwich	•	•	•		•	•	•	•	
Luo et al. [136]	2011	Polymer sandwich	•	•	•	•			•		•

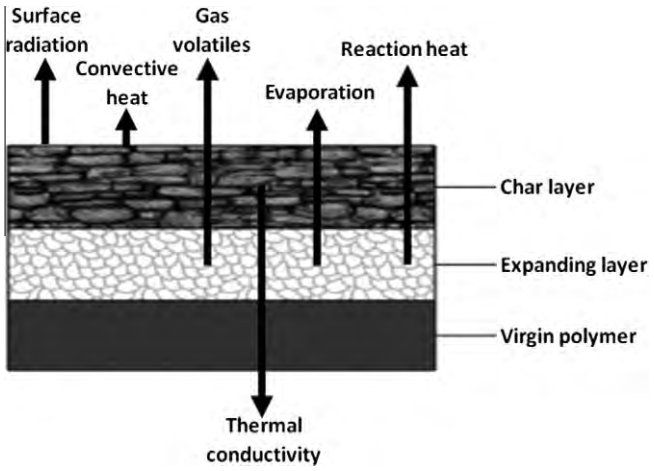

Fig. 7. Fire processes of intumescent polymers under external heat flux.

degrades during this stage; (ii) intumescence – components within the coating decomposes to produce large amounts of gas of which some fraction is trapped within the molten matrix; (iii) char formation – the molten fluid hardens and releases residual volatile components, and (iv) char degradation – the char layer oxidizes or pyrolyzes leaving only an inert, porous matrix. Fire processes of intumescent polymers under external heat flux are shows in Fig. 7. Solid phase of intumescent polymers can be divided into three layers: char layer, expanding layer and virgin polymer.

Table 15 shows a summary of considerations in previous one-dimensional models for intumescent polymers. It is noticed that all of the models have considered heat conduction, pyrolysis reaction, production of gas volatiles and expansion. Based on reviewed papers, however, very few models have been found considered mechanical behaviors when intumescent polymers were positioned under heating and loading. Modeling of mechanical behaviors of intumescent polymers are very complicated because of irregular expansions.

4. Conclusions

This paper presents a critical review of fire processes modeling of combustible materials under external heat flux, including woods, non-charring polymers, charring polymers and intumescent polymers. To improve modeling accuracy and expand application fields, several aspects are needed to be noticed in future work:

(1) Although thermal, chemical and physical processes was often included in one-dimensional modeling, attentions are needed to be paid on prediction of toxic gases. Many models have considered gas volatiles, but description usually focused on the production of a mixture of gas volatiles. Individual gas volatiles, such as CO, CO_2, H_2O, are needed to be investigated. Transportation of gas volatiles inside solid phase were sometimes ignored. To improve modeling accuracy, several considerations such as volume change, water evaporation, internal gas pressure, and temperature dependent thermal properties are needed to be taken.

(2) Statistics shows a relative lack of studies on mechanical behaviors of woods, non-charring and intumescent polymers. As a popular structure material, woods have rarely been studied on modeling of mechanical behaviors. Although non-charring and intumescent polymers are less used as structure elements, thermal properties and other fire behaviors would be different under loading. And decorative materials made by these polymers may have influence on fire structure. Some models have considered mechanical behavior of charring polymers, but modeling accuracy and applications are affected because of limited empirical models or experimental data.

(3) Experimental data and empirical models are needed to describe fire processes of combustible materials. Although Arrhenius equation was largely used to describe pyrolysis reactions and water evaporation, applications are limited because of limited experimental data of describing production of gas volatiles and water evaporation process. Thermal

Table 15
A summary of considerations in previous one-dimensional models for intumescent polymers.

Models	Year	Material	Heat conduction	Pyrolysis	Gas volatiles	Volume change	Internal gas pressure	Water evaporation	Permeability	Porosity	Mechanical behaviors
Anderson et al. [137,202]	1984	Coating	•	•	•	•					
Buckmaster et al. [138]	1986	Coating	•	•	•	•					
Henderson and Wiecek [23,102]	1987	$H_{41}N$	•	•	•	•	•		•	•	
Florio et al. [139]	1991	$H_{41}N$	•	•	•	•	•		•	•	
Looyeh et al. [203]	1997	GRP panel	•	•	•						
Shih et al. [140]	1998	Coating	•	•	•	•	•		•	•	
Dodds et al. [204]	2000	GRP panel	•	•	•						
Bhargava et al. [142]	2000	Epoxy composite	•	•		•					
Stagges [131,208,209]	2000	PVC	•	•	•	•	•		•	•	
Di Blasi and Branca [144]	2001	Coating	•	•	•	•	•			•	
Di Blasi [145]	2004	Coating	•	•	•	•	•			•	
Gibson et al. [151]	2006	Polyester/E-glass	•	•	•						•
Bahramian et al. [132]	2006	Phenolic resin	•	•	•	•	•			•	
Trelles and Lattimer [205]	2007	Phenolic composite	•	•	•						
Feih et al. [20,133,152]	2007	Vinyl ester	•	•	•	•					•
Bai et al. [153,206]	2008	FRP	•	•	•	•					•
Farkas et al. [207]	2008	Epoxy resin	•	•	•		•		•	•	
Lautenberger and Fernandez-Pello [21,135]	2009	Coating	•	•	•	•	•	•	•	•	
Griffin [146]	2010	Coating	•	•	•	•	•			•	
Stoliarov et al. [4]	2010	PC, PVC	•	•	•	•	•	•		•	

properties in some previous models are considered temperature independent. To improve the modeling accuracy, experimental data for temperature dependent thermal properties are critically important.

Integrated model which can describe all four fire processes for different species of combustible materials is significant to improve modeling accuracy and expand application fields of complicated fire. An integrated one-dimensional model with high modeling accuracy will be an impulsive force to two- and three-dimensional modeling of building fires.

References

[1] Janssens M, Douglas B. Wood and wood products. In: Handbook of building materials for fire protection. New York: McGraw-Hill; 2004. p. 7.1–7.58.
[2] Di Blasi C. Transition between regimes in the degradation of thermoplastic polymers. Polym Degrad Stab 1999;64:359–67.
[3] Sullivan RM, Salamon NJ. A finite element method for the thermochemical decomposition of polymeric materials – II. Carbon phenolic composites. Int J Eng Sci 1992;30:939–51.
[4] Stoliarov SI, Crowley S, Walters RN, Lyon RE. Prediction of the burning rates of charring polymers. Combust Flame 2010;157:2024–34.
[5] Spearpoint MJ, Quintiere JG. Predicting the piloted ignition of wood in the cone calorimeter using an integral model-effect of species, grain orientation and heat flux. Fire Saf J 2001;36:391–415.
[6] Mouritz AP, Feih S, Kandare E, Mathys Z, Gibson AG, Des Jardin PE, et al. Review of fire structural modelling of polymer composites. Composites A 2009;40:1800–14.
[7] Tinney ER. The combustion of wooden dowels in heated air. Symp (Int) Combust 1965;10:925–30.
[8] Kung HC. A mathematical model of wood pyrolysis. Combust Flame 1972;18:185–95.
[9] Perre P. Measurements of softwoods' permeability to air: importance upon the drying model. Int Commun Heat Mass Transfer 1987;14:519–29.
[10] Aerts PDJ, Rageland KW. Pressurized downdraft combustion of woodchips. In: Twenty-third symposium (international) on combustion, Pittsburgh, USA; 1990. p. 1025–32.
[11] McManus HLN, Springer GS. High temperature thermomechanical behavior of carbon–phenolic and carbon–carbon composites, I. Analysis. J Compos Mater 1992;26:206–29.
[12] Quintiere JG. A semi-quantitative model for the burning rate of solid materials. Final report. Report No.: NISTIR 4840. National Institute of Standard Technology (NIST); 1992.
[13] Di Blasi C. Numerical simulation of cellulose pyrolysis. Biomass Bioenergy 1994;7:87–98.
[14] Staggs JEJ. A discussin of modelling idealised ablative materials with particular reference to fire testing. Fire Saf. J. 1996;28:47–66.
[15] Moghtaderi B, Novozhilov V, Fletcher D, Kent JH. An integral model for the transient pyrolysis of solid materials. Fire Mater. 1997;21:7–16.
[16] Spearpoint MJ. Predicting the ignition and burning rate of wood in the cone calorimeter using an integral model. Master thesis. University of Maryland, College Park; 1999.
[17] Babu BV, Chaurasia AS. Modeling for pyrolysis of solid particle: kinetics and heat transfer effects. Energy Convers Manage 2003;44:2251–75.
[18] Gibson AG, Wright PNH, Wu YS. The integrity of polymer composites during and after fire. J Compos Mater 2004;38:1283–307.
[19] Gu P, Asaro RJ. Structural buckling of polymer matrix composites due to reduced stiffness from fire damage. Compos Struct 2005;69:65–75.
[20] Feih S, Mouritz AP, Mathys Z, Gibson AG. Tensile strength modeling of glass fiber–polymer composites in fire. J Compos Mater 2007;41:2387–410.
[21] Lautenberger C. A generalized pyrolysis model for combustible solids. PhD thesis. Berkeley: University of California; 2007.
[22] Stoliarov SI, Lyon RE. Thermo-kinetic model of burning for pyrolyzing materials. In: The ninth international symposium on fire safety science, German; 2008. p. 38–50.
[23] Henderson JB, Wiecek TE. A mathematical model to predict the thermal response of decomposing, expanding polymer composites. J Compos Mater 1987;21:373–93.
[24] Alves SS, Figueiredo JL. A model for pyrolysis of wet wood. Chem Eng Sci 1989;44:2861–9.
[25] Parker WJ. Prediction of the heat release rate of wood. In: The first international symposium on fire safety science, MA, USA; 1986. p. 207–16.
[26] White RH, Schaffer EL. Application of CMA program to wood charring. Fire Technol. 1978;14:279–90.
[27] Fan LT, Fan LS, Miyanami K, Chen TY, Walawender WP. A mathematical model for pyrolysis of a solid particle. Can J Chem Eng 1977;55:47–53.
[28] Kansa EJ, Perlee HE, Chaiken RF. Mathematical model of wood pyrolysis including internal forced convection. Combust Flame 1977;29:311–24.
[29] Hallman JR, Welker JR, Sliepcevich CM. Polymer surface reflectance–absorptance characteristics. Polym Eng Sci 1974;14:717–23.
[30] Wesson HR, Welker JR, Sliepcevich CM. The piloted ignition of wood by thermal radiation. Combust Flame 1971;16:303–10.
[31] Park WC, Atreya A, Baum HR. Experimental and theoretical investigation of heat and mass transfer processes during wood pyrolysis. Combust Flame 2010;157:481–94.
[32] Mohan D, Pittman CU, Steele PH. Pyrolysis of wood/biomass for bio-oil: a critical review. Energy Fuels 2006;20:848–89.
[33] Varhegyi G, Antal MJ, Szekely T, Szabo P. Kinetics of the thermal decomposition of cellulose, hemicellulose, and sugarcane bagasse. Energy Fuels 1989;3:329–35.
[34] Capart R, Khezami L, Burnham AK. Assessment of various kinetic models for the pyrolysis of a microgranular cellulose. Thermochim Acta 2004;417:79–89.
[35] Chan RWC, Krieger BB. Kinetics of dielectric-loss microwave degradation of polymers: lignin. J Appl Polym Sci 1981;26:1533–53.
[36] Kilzer FJ, Broido A. Speculation on the nature of cellulose pyrolysis. Pyrodynamics 1965;2:151–63.
[37] Tihay V, Boulnois C, Gillard P. Influence of oxygen concentration on the kinetics of cellulose wadding degradation. Thermochim Acta 2011;525:16–24.
[38] Martin-Gullon I, Esperanza M, Font R. Kinetic model for the pyrolysis and combustion of poly-(ethylene terephthalate) (PET). J Anal Appl Pyrolysis 2001;58–59:635–50.
[39] Shi L, Chew MYL, Xie QY, Zhang RF, Li LM, Xu CM. Experimental study on fire characteristics of PC monitors – Part I: combustion properties and pyrolysis characteristics. J Appl Fire Sci 2010;19:23–39.
[40] Samolada MC, Vasalos IA. A kinetic approach to the flash pyrolysis of biomass in a fluidized bed reactor. Fuel 1991;70:883–9.
[41] Wagenaar BM, Prins W, Van Swaaij WPM. Flash pyrolysis kinetics of pine wood. Fuel Process Technol 1993;36:291–8.
[42] Chan WCR, Kelbon M, Krieger BB. Modelling and experimental verification of physical and chemical processes during pyrolysis of a large biomass particle. Fuel 1985;64:1505–13.
[43] Liu NA, Fan WC. Modelling the thermal decompositions of wood and leaves under a nitrogen atmosphere. Fire Mater 1998;22:103–8.
[44] Thurner F, Mann U. Kinetic investigation of wood pyrolysis. Ind Eng Chem Process Des Dev 1981;20:482–8.
[45] Di Blasi C. Modeling chemical and physical processes of wood and biomass pyrolysis. Prog Energy Combust Sci 2008;34:47–90.
[46] Nunn TR, Howard JB, Longwell JP, Peters WA. Product compositions and kinetics in the rapid pyrolysis of sweet gum hardwood. Ind Eng Chem Process Des Dev 1985;24:836–44.
[47] Swann J, Hartman J, Beyler C. Study of radiant smoldering ignition of plywood subjected to prolonged heating using the cone calorimeter, TGA, and DSC. In: The ninth international symposium on fire safety science, German; 2008. p. 98–102.
[48] Stoliarov SI, Crowley S, Lyon RE, Linteris GT. Prediction of the burning rates of non-charring polymers. Combust Flame 2009;156:1068–83.
[49] Kang BS, Kim SG, Kim JS. Thermal degradation of poly(methyl methacrylate) polymers: kinetics and recovery of monomers using a fluidized bed reactor. J Anal Appl Pyrolysis 2008;81:7–13.
[50] Bockhorn H, Hornung A, Hornung U, Lochner S. Pyrolysis of polystyrene as the initial step in incineration, fires, or smoldering of plastics: investigations of the liquid phase. Proc Combust Inst 2000;28:2667–73.
[51] Carniti P, Beltrame PL, Armada M, Gervasini A, Audisio G. Polystyrene thermodegradation. 2. Kinetics of formation of volatile products. Ind Eng Chem Res 1991;30:1624–9.
[52] Liu YR, Guo SH, Qian JL. Study on the decomposition kinetics of polystyrene by using sequential pyrolysis gas chromatograph. Pet Sci Technol 1999;17:1089–105.
[53] Westerhout RWJ, Waanders J, Kuipers JAM, Van Swaaij WPM. Kinetics of the low-temperature pyrolysis of polyethene, polypropene, and polystyrene modeling, experimental determination, and comparison with literature models and data. Ind Eng Chem Res 1997;36:1955–64.
[54] Ciutacu S, Fatu D, Segal E. On the thermal stability of some macromolecular compounds. Thermochim Acta 1988;131:279–84.
[55] Kannan P, Biernacki JJ, Visco DP. A review of physical and kinetic models of thermal degradatin of expanded polystyrene foam and their application to the lost foam casting process. J Anal Appl Pyrolysis 2007;78:162–71.
[56] Grammelis P, Basinas P, Malliopoulou A, Sakellaropoulos G. Pyrolysis kinetics and combustion characteristics of waste recovered fuels. Fuel 2009;88:195–205.
[57] Simon P. Kinetics of polymer degradation involving the splitting off of small molecules: Part 7 – thermooxidative dehydrochlorination of PVC. Polym Degrad Stab 1992;36:85–9.
[58] Bockhorn H, Hornung A, Hornung U. Mechanisms and kinetics of thermal decomposition of plastics from isothermal and dynamic measures. J Anal Appl Pyrolysis 1999;50:77–101.
[59] Saastamoinen J, Tourunen A. Model for char combustion, particle size distribution, and inventory in air and oxy-fuel combustion in fluidized beds. Energy Fuels 2012;26:407–16.
[60] Saastamoinen J, Aho M, Moilanen A, Sorensen LH, Clausen S, Berg M. Burnout of pulverized biomass particles in large scale boiler – single particle model approach. Biomass Bioenergy 2010;34:728–36.
[61] Saastamoinen J. Modelling of dynamics of combustion of biomass in fluidized beds. Therm Sci 2004;8:107–26.

[62] Saastamoinen JJ, Aho MJ, Hamalainen JP, Hernberg R, Joutsenoja T. Pressurized pulverized fuel combustion in different concentrations of oxygen and carbon dioxide. Energy Fuels 1996;10:121–33.
[63] Saastamoinen JJ, Aho MJ, Linna VL. Simultaneous pyrolysis and char combustion. Fuel 1993;72:599–609.
[64] Kaushal P, Proll T, Hofbauer H. Model development and validation: co-combustion of residual char, gases and volatile fuels in the fast fluidized combustion chamber of a dual fluidized bed biomass gasifier. Fuel 2007;86:2687–95.
[65] Williams A, Jones JM, Ma L, Pourkashanian M. Pollutants from the combustion of solid biomass fuels. Prog Energy Combust Sci 2012;38:113–37.
[66] Di Blasi C. Combustion and gasification rates of lignocellulosic chars. Prog Energy Combust Sci 2009;35:121–40.
[67] Williams A, Pourkashanian M, Jones JM. Combustion of pulverised coal and biomass. Prog Energy Combust Sci 2001;27:587–610.
[68] Hurt RH, Calo JM. Semi-global intrinsic kinetics for char combustion modeling. Combust Flame 2001;125:1138–49.
[69] Bews IM, Hayhurst AN, Richardson SM, Taylor SG. The order, Arrhenius parameters, and mechanism of the reaction between gaseous oxygen and solid carbon. Combust Flame 2001;124:231–45.
[70] Smith IW. The combustion rates of coal chars: a review. Symp (Int) Combust 1982;19:1045–65.
[71] Laurendeau NM. Heteogeneous kinetics of coal char gasification and combustion. Prog Energy Combust Sci 1978;4:221–70.
[72] Arthur JR. Reactions between carbon and oxygen. Trans Faraday Soc 1951;47:164–78.
[73] Tognotti L, Longwell JP, Sarofim. The products of the high temperature oxidation of a single char particle in an electrodynamic balance. Symp (Int) Combust 1991;23:1207–13.
[74] Murphy JJ, Shaddix CR. Combustion kinetics of coal chars in oxygen-enriched environments. Combust Flame 2006;144:710–29.
[75] Pitts WM. The global equivalence ratio concept and the formation mechanisms of carbon monoxide in enclosure fires. Prog Energy Combust Sci 1995;21:197–237.
[76] He F, Behrendt F. A new method for simulating the combustion of a large biomass particle – a combination of a volume reaction model and front reaction approximation. Combust Flame 2011;158:2500–11.
[77] Shi L, Chew MYL. Experimental study of carbon monoxide for woods under spontaneous ignition condition. Fuel 2012;102:709–15.
[78] Font R, Marcilla A, Verdu E, Devesa J. Kinetics of the pyrolysis of almond shells and almond shells impregnated with cobalt dichloride in a fluidized bed reactor and in a pyroprobe 100. Ind Eng Chem Res 1990;29:1846–55.
[79] Scott DS, Piskorz J, Radlein D. Liquid products from the continuous flash pyrolysis of biomass. Ind Eng Chem Process Des Dev 1985;24:581–8.
[80] Shi L, Chew MYL. A model to predict carbon monoxide of woods under external heat flux – Part I: theory. In: The 9th Asia–Oceania symposium on fire science and technology, Hefei, China; in press.
[81] Shi L, Chew MYL. A model to predict carbon monoxide of woods under external heat flux – Part II: validation and application. In: The 9th Asia–oceania symposium on fire science and technology, Hefei, China; in press.
[82] Grotkjær T, Dam-Johansen K, Jensen AD, Glarborg P. An experimental study of biomass ignition. Fuel 2003;82:825–33.
[83] Ragland KW, Aerts DJ. Properties of wood for combustion analysis. Bioresour Technol 1991;37:161–8.
[84] Wang HY. Prediction of soot and carbon monoxide production in a ventilated tunnel fire by using a computer simulation. Fire Saf J 2009;44:394–406.
[85] Floyd JE, McGrattan KB. Extending the mixture fraction concept to address under-ventilated fire. Fire Saf J 2009;44:291–300.
[86] Saastamoinen JJ, Kilpinen PT, Norstrom TN. New simplified rate equation for gas-phase CO oxidation at combustion. Energy Fuels 2000;14:1156–60.
[87] Li K, You CF. Particle combustion model simultaneously considering a volatile and carbon reaction. Energy Fuels 2010;24:4178–84.
[88] Gomez-Barea A, Leckner B. Modeling of biomass gasification in fluidized bed. Prog Energy Combust Sci 2010;36:444–509.
[89] Eslami A, Sohi AH, Sheikhi A, Sotudeh-Gharebagh R. Sequential modeling of coal volatile combustion in fluidized bed reactors. Energy Fuels 2012;26:5199–209.
[90] Srinivasan RA, Sriramulu S, Kulasekaran S, Agarwal PK. Mathematical modeling of fluidized bed combustion – 2: combustion of gases. Fuel 1998;77:1022–49.
[91] Ravelli S, Perdichizzi A, Barigozzi G. Description, applications and numerical modelling of bubbling fluidized bed combustion in waste-to-energy plants. Prog Energy Combust Sci 2008;34:224–53.
[92] Hannes JP. Mathematical modeling of circulating fluidized bed combustion. PhD thesis. Bibliotheek Technische Universiteit; 1996.
[93] Williams FA. Progress in knowledge of flamelet structure and extinction. Prog Energy Combust Sci 2000;26:657–82.
[94] Pitsch H, Chen M, Peters N. Unsteady flamelet modeling of turbulent hydrogen-air diffusion flames. Symp (Int) Combust 1998;27:1057–64.
[95] Jones JM, Patterson PM, Pourkashanian M, Rowlands L, Williams A. An advanced coal model to predict NOx formation and carbon burnout in pulverised coal flames. In: The 14th annual international pittsburgh coal conference, Taiyuan, China; 1997.
[96] Galgano A, Di Blasi C, Milella E. Sensitivity analysis of a predictive model for the fire behaviour of a sandwich panel. Polym Degrad Stab 2010; 95:2430–44.
[97] Ratte J, Marias F, Vaxelaire J, Bernada P. Mathematical modelling of slow pyrolysis of a particle of treated wood waste. J Hazard Mater 2009;170: 1023–40.
[98] Lautenberger C, Fernandez-Pello C. A model for the oxidative pyrolysis of wood. Combust Flame 2009;156:1503–13.
[99] Vijeu R, Gerun L, Tazerout M, Castelain C, Bellettre J. Dimensional modelling of wood pyrolysis using a nodal approach. Fuel 2008;87: 3292–303.
[100] Wang YF, Yang LZ, Zhou XD, Dai JK, Zhou YP, Deng ZH. Experiment study of the altitude effects on spontaneous ignition characteristics of wood. Fuel 2010;89:1029–34.
[101] Di Blasi C. Heat, momentum and mass transport through a shrinking biomass particle exposed to thermal radiation. Chem Eng Sci 1996;51:1121–32.
[102] Henderson JB, Wiecek TE. A numerical study of the thermally-induced response of decomposing, expanding polymer composites. Warme- und Stoffubertragung 1988;22:275–84.
[103] Hastaoglu MA, Berruti F. A gas-solid reaction model for flash wood pyrolysis. Fuel 1989;68:1408–15.
[104] Lede J. Reaction temperature of solid particles undergoing an endothermal volatilization: application to the fast pyrolysis of biomass. Biomass Bioenergy 1994;7:49–60.
[105] Hastaoglu MA, Hassam MS. Application of a general gas-solid reaction model to flash pyrolysis of wood in a circulating fluidized bed. Fuel 1994;74:697–703.
[106] Larfeldt J, Leckner B, Melaaen MC. Modelling and measurements of the pyrolysis of large wood particles. Fuel 2000;79:1637–43.
[107] Di Blasi C. Modeling intra- and extra-particle processes of wood fast pyrolysis. AIChE J 2002;48:2386–97.
[108] Hagge MJ, Bryden KM. Modeling the impact of shrinkage on the pyrolysis of dry biomass. Chem Eng Sci 2002;57:2811–23.
[109] Klose W, Schinkel A. Measurement and modelling of the development of pore size distribution of wood during pyrolysis. Fuel Process Technol 2002;77–78:459–66.
[110] Bryden KM, Ragland KW, Rutland C. Modeling thermally thick pyrolysis of wood. Biomass Bioenergy 2002;22:41–53.
[111] Bruch C, Peters B, Nussbaumer T. Modelling wood combustion under fixed bed conditions. Fuel 2003;82:729–38.
[112] Bellais M, Davidsson KO, Liliedahl T, Sjostrom K, Pettersson JBC. Pyrolysis of large wood particles: a study of shrinkage importance in simulations. Fuel 2003;82:1541–8.
[113] Galgano A, Di Blasi C. Modeling the propagation of drying and decomposition fronts in wood. Combust Flame 2004;139:16–27.
[114] Theuns E, Merci B, Vierendeels J, et al. Extension and evaluation of the integral model for transient pyrolysis of charring materials. Fire Mater 2005;29:195–212.
[115] Yang YB, Phan AN, Ryu C, Sharifi V, Swithenbank J. Mathematical modelling of slow pyrolysis of segregated solid wastes in a packed-bed pyrolyser. Fuel 2007;86:169–80.
[116] Sadhukhan AK, Gupta P, Saha RK. Modelling and experimental studies on pyrolysis of biomass particles. J Anal Appl Pyrolysis 2008;81: 183–92.
[117] Larfeldt J, Leckner B, Melaaen MC. Modelling and measurements of drying and pyrolysis of large wood particles. In: Progress in thermochemical biomass conversion; 2008. p. 1046–60.
[118] Tran HC, White RH. Burning rate of solid wood measured in a heat release rate calorimeter. Fire Mater 1992;16:197–206.
[119] Raji S, Jannot Y, Lagiere P, Puiggali JR. Thermophysical characterization of a laminated solid-wood pine wall. Constr Build Mater 2009;23: 3189–95.
[120] Anne Palin M, Petty JA. Permeability to water of the wood cell wall and its variation with temperature. Wood Sci Technol 1983;17:187–93.
[121] Wang JM, Dai CY, Liu YX. Wood permeability. J For Res 1991;2:91–7.
[122] Pauly S. Permeability and diffusion data. In: Polymer handbook. New York: John Wiley & Sons; 2003. p. 435–49.
[123] Shi L, Chew MYL. Influence of moisture on autoignition of woods in cone calorimeter. J Fire Sci 2012;30:158–69.
[124] Shi L, Chew MYL. Experimental study of woods under external heat flux by autoignition: ignition time and mass loss rate. J Therm Anal Calorim 2012. http://dx.doi.org/10.1007/s10973-012-2489-x.
[125] Gronli MG. A theoretical and experimental study of the thermal degradation of biomass. PhD thesis. The Norwegian University of Science and Technology; 1996.
[126] Sand U, Sandberg J, Larfeldt J, Fdhila RB. Numerical prediction of the transport and pyrolysis in the interior and surrounding of dry and wet wood log. Appl Energy 2008;85:1208–24.
[127] MatWeb. Database of material properties; 2011. <www.matweb.com>.
[128] Starzhenetskaya TA, Davydova NN. Investigation of the effect of moisture on polymer composites by the method of thermogravimetry. J Eng Phys Thermophys 1999;72:106–8.
[129] Peters B, Bruch C. A flexible and stable numerical method for simulating the thermal decomposition of wood particles. Chemosphere 2001;42: 481–90.
[130] Sullivan RM, Salamon NJ. A finite element method for the thermochemical decomposition of polymeric materials – I. Theory. Int J Eng Sci 1992;30:431–41.

[131] Staggs JEJ. A simple model of polymer pyrolysis including transport of volatiles. Fire Saf J 2000;34:69–80.
[132] Bahramian AR, Kokabi M, Famili MHN, Beheshty MH. Ablation and thermal degradation behaviour of a composite based on resol type phenolic resin: process modeling and experimental. Polymer 2006;47: 3661–73.
[133] Feih S, Mathys Z, Gibson AG, Mouritz AP. Modelling the compression strength of polymer laminates in fire. Composites A 2007;38:2354–65.
[134] Gu P, Asaro RJ. Designing sandwich polymer matrix composite panels for structural integrity in fire. Compos Struct 2009;88:461–7.
[135] Lautenberger C, Fernandez-Pello C. Generalized pyrolysis model for combustible solids. Fire Saf J 2009;44:819–39.
[136] Luo CS, Lue J, DesJardin PE. Thermo-mechanical damage modeling of polymer matrix sandwich composites in fire. Composites A 2011. http://dx.doi.org/10.1016/j.compositesa.2011.03.006.
[137] Anderson CE, Wauters DK. A thermodynamic heat transfer model for intumescent systems. Int J Eng Sci 1984;22:881–9.
[138] Buckmaster J, Anderson C, Nachman A. A model for intumescent paints. Int J Eng Sci 1986;24:263–76.
[139] Florio J, Henderson JB, Test FL, Hariharan R. A study of the effects of the assumption of local-thermal equilibrium on the overall thermally-induced response of a decomposing glass-filled polymer composite. Int J Heat Mass Transfer 1991;34:135–47.
[140] Shih YC, Cheung FB, Koo JH. Theoretical modeling of intumescent fire-retardant materials. J Fire Sci 1998;16:46–71.
[141] Bourbigot S, Duquesne S, Leroy JM. Modeling of heat transfer of a polypropylene-based intumescent system during combustion. J Fire Sci 1999;17:42–56.
[142] Bhargava A, Griffin GJ, Green JCA. A model of heat transfer across an epoxy based fire retardant layer undergoing sublimation, intumescence and degradation. Dev Chem Eng Miner Process 2000;8:75–91.
[143] Zhou Y, Fernandez-Pello AC. Numerical modeling of endothermic pyrolysis and ignition delay of composite materials exposed to an external radiant heat flux. Proc Combust Inst 2000;28:2769–75.
[144] Di Blasi C, Branca C. Mathematical model for the nonsteady decomposition of intumescent coatings. AIChE J 2001;47:2359–70.
[145] Di Blasi C. Modeling the effects of high radiative heat fluxes on intumescent material decomposition. J Anal Appl Pyrolysis 2004;71:721–37.
[146] Griffin GJ. The modeling of heat transfer across intumescent polymer coatings. J Fire Sci 2010;28:249–77.
[147] Klason C, Kubat J, De Ruvo A. Radiometric investigations on thermal expansion and transitions in polymers. Rheol Acta 1967;6:390–6.
[148] Murthy NM, Rani Rao D. Effect of X-ray irradiation on the thermal expansion of polymers. J Mater Sci 1986;21:1206–10.
[149] Suleiman BM, Larfeldt J, Leckner B, Gustavsson M. Thermal conductivity and diffusivity of wood. Wood Sci Technol 1999;33:465–73.
[150] De Souza Costa F, Sandberg D. Mathematical model of a smoldering log. Combust Flame 2004;139:227–38.
[151] Gibson AG, Wu YS, Evans JT. Laminate theory analysis of composites under load in fire. J Compos Mater 2006;40:639–58.
[152] Feih S, Mathys Z, Gibson AG, Mouritz AP. Modelling the tension and compression strengths of polymer laminates in fire. Compos Sci Technol 2007;67:551–64.
[153] Bai Y, Keller T. Modeling of mechanical response of FRP composites in fire. Composites A 2009;40:731–8.
[154] Mouritz AP, Mathys Z. Post-fire mechanical properties of glass-reinforced polyester composites. Compos Sci Technol 2001;61:475–90.
[155] McManus HLN, Springer GS. High temperature thermomechanical behavior of carbon–phenolic and carbon–carbon composites, II. Results. J Compos Mater 1992;26:230–55.
[156] Elmughrabi AE, Robinson M, Gibson AG. Effect of stress on the fire reaction properties of polymer composite laminates. Polym Degrad Stab 2008;93:1877–83.
[157] Cachim PB, Franssen JM. Comparison between the charring rate model and the conductive model of Eurocode 5. Fire Mater 2009;33:129–43.
[158] Hadvig S, Paulsen O. One dimensional charring rates in wood. J Fire Flammab 1976;7:433–49.
[159] Panton RL, Rittmann JG. Pyrolysis of a slab of porous material. Symp (Int) Combust 1971;13:881–91.
[160] Sibulkin M. Heat of gasification for pyrolysis of charring materials. In: The first international symposium on fire safety science, MA, USA; 1986. p. 391–400.
[161] Capart R, Falk L, Gelus M. Pyrolysis of wood macrocylinders under pressure: application of a simple mathematical model. Appl Energy 1988;30:1–13.
[162] Koufopanos CA, Papayannakos N, Maschio G, Lucchesi A. Modelling of the pyrolysis of biomass particles: studies on kinetics, thermal and heat transfer effects. Can J Chem Eng 1991;69:907–15.
[163] Fredlund B. Modelling of heat and mass transfer in wood structures during fire. Fire Saf J 1993;20:39–69.
[164] Shrestha D, Cramer S, White R. Time–temperature profile across a lumber section exposed to pyrolytic temperatures. Fire Mater 1994;18: 211–20.
[165] Wagenaar BM, Prins W, Van Swaaij WPM. Pyrolysis of biomass in the rotating cone reactor: modelling and experimental justification. Chem Eng Sci 1994;49:5109–26.
[166] Di Blasi C. Kinetic and heat transfer control in the slow and flash pyrolysis of solids. Ind Eng Chem Res 1996;35:37–46.
[167] Saastamoinen J, Richard JR. Simultaneous drying and pyrolysis of solid fuel particles. Combust Flame 1996;106:288–300.
[168] Ahuja P, Kumar S, Singh PC. A model for primary and heterogeneous secondary reactions of wood pyrolysis. Chem Eng Technol 1996; 19:272–82.
[169] Bilbao R, Mastral JF, Ceamanos J, Aldea ME. Modelling of the pyrolysis of wet wood. J Anal Appl Pyrolysis 1996;36:81–97.
[170] Moghtaderi B, Dlugogorski BZ, Kennedy EM, Fletcher DF. Effects of the structural properties of solid fuels on their re-ignition characteristics. Fire Mater 1998;22:155–65.
[171] Jia F, Galea ER, Patel MK. Numerical simulation of the mass loss process in pyrolizing char materials. Fire Mater 1999;23:71–8.
[172] Janse AMC, Westerhout RWJ, Prins W. Modelling of flash pyrolysis of a single wood particle. Chem Eng Process 2000;39:239–52.
[173] Gronli MG, Melaaen MC. Mathematical model for wood pyrolysis – comparison of experimental measurements with model predictions. Energy Fuels 2000;14:791–800.
[174] Spearpoint MJ, Quintiere JG. Predicting the burning of wood using an integral model. Combust Flame 2000;123:308–24.
[175] Peters B, Bruch C. Drying and pyrolysis of wood particles: experiments and simulation. J Anal Appl Pyrolysis 2003;70:233–50.
[176] Mousques P, Dirion JL, Grouset D. Modeling of solid particles pyrolysis. J Anal Appl Pyrolysis 2001;58–59:733–45.
[177] Babu BV, Chaurasia AS. Modeling, simulation and estimation of optimum parameters in pyrolysis of biomass. Energy Convers Manage 2003;44:2135–58.
[178] Babu BV, Chaurasia AS. Pyrolysis of biomass: improved models for simultaneous kinetics and transport of heat, mass and momentum. Energy Convers Manage 2004;45:1297–327.
[179] Babu BV, Chaurasia AS. Heat transfer and kinetics in the pyrolysis of shrinking biomass particle. Chem Eng Sci 2004;59:1999–2012.
[180] Bellais M. Modelling of the pyrolysis of large wood particles. PhD thesis. Royal Institute of Technology; 2007.
[181] Janssens ML. Modeling of the thermal degradation of structural wood members exposed to fire. Fire Mater 2004;28:199–207.
[182] Theuns E, Merci B, Vierendeels J, et al. Critical evaluation of an integral model for the pyrolysis of charring materials. Fire Saf J 2005; 40:121–40.
[183] Shen DK, Fang MX, Luo ZY, Cen KF. Modeling pyrolysis of wet wood under external heat flux. Fire Saf J 2007;42:210–7.
[184] Sadhukhan AK, Gupta P, Saha RK. Modelling of pyrolysis of large wood particles. Bioresour Technol 2009;100:3134–9.
[185] Craft ST, Isgor B, Hadjisophocleous G, Mehaffey JR. Predicting the thermal response of gypsum board subjected to a constant heat flux. Fire Mater 2008;32:333–55.
[186] Grieco E, Baldi G. Analysis and modelling of wood pyrolysis. Chem Eng Sci 2011;66:650–60.
[187] Dufour A, Ouartassi B, Bounaceur R, Zoulalian A. Modelling intra-particle phenomena of biomass pyrolysis. Chem Eng Res Des 2011;89:2136–46.
[188] Di Blasi C, Crescitelli S, Russo G, Cinque G. Numerical model of ignition processes of polymeric materials including gas-phase absorption of radiation. Combust Flame 1991;83:333–44.
[189] Di Blasi C. Modeling and simulation of combustion processes of charring and non-charring solid fuels. Prog Energy Combust Sci 1993; 19:71–104.
[190] Quintiere JG, Iqbal N. An approximater integral model for the burning rate of a thermoplastic-like material. Fire Mater 1994;18:89–98.
[191] Di Blasi C. Modeling of solid- and gas-phase processes during thermal degradation of composite materials. Polym Degrad Stab 1996; 54:241–8.
[192] Staggs JEJ. Modelling thermal degradation of polymers using single-step first-order kinetics. Fire Saf J 1999;32:17–34.
[193] Staggs JEJ. A simplified mathematical model for the pyrolysis of polymers with inert additives. Fire Saf J 1999;32:221–40.
[194] Zhou YY, Walther DC, Fernandez-Pello AC. Numerical analysis of piloted ignition of polymeric materials. Combust Flame 2002;131:147–58.
[195] Esfahani JA, Kashani A. One-dimensional numerical model for degradation and combustion of polymethyl methacrylate. Heat Mass Transfer 2006;42:569–76.
[196] Rein G. From pyrolysis kinetics to models of condensed-phase burning. Recent Adv Flame Retard Polym Mater 2008;19:56–65.
[197] Bal N, Rein G. Numerical investigation of the ignition delay time of a translucent solid at high radiant heat fluxes. Combust Flame 2011; 158:1109–16.
[198] Chaos M, Khan MM, Krishnamoorthy N, De Ris JL, Dorofeev SB. Evaluation of optimization schemes and determination of solid fuel properties for CFD fire models using bench-scale pyrolysis tests. Proc Combust Inst 2011; 33:2599–606.
[199] Di Blasi C. Linear pyrolysis of cellulosic and plastic waste. J Anal Appl Pyrolysis 1997;40–41:463–79.
[200] Krysl P, Ramroth WT, Stewart LK, Asaro RJ. Finite element modelling of fibre reinforced polymer sandwich panels exposed to heat. Int J Numer Methods Eng 2004;61:49–68.

[201] Salvador S, Qunintard M, David C. Combustion of a substitution fuel made of cardboard and polyethylene: influence of the mix characteristics – modelling. Fire Mater 2008;32:417–44.
[202] Anderson CE, Dziuk JJ, Mallow JWA. Intumescent reaction mechanisms. J Fire Sci 1985;3:161–94.
[203] Looyeh MRE, Bettess P, Gibson AG. A one-dimensional finite element simulation for the fire-performance of GRP panels for offshore structures. Int J Numer Methods Heat Fluid Flow 1997;7:609–25.
[204] Dodds N, Gibson AG, Dewhurst D, Davies JM. Fire behaviour of composite laminates. Composites A 2000;31:689–702.
[205] Trelles J, Lattimer BY. Modelling thermal degradation of composite materials. Fire Mater 2007;31:147–71.
[206] Bai Y, Vallee T, Keller T. Modeling of thermal responses for FRP composites under elevated and high temperatures. Compos Sci Technol 2008;68:47–56.
[207] Farkas E, Meszena ZG, Toldy A, Matko S, Marosfoi BB, Marosi G. Modelling of transport processes in a developing char. Polym Degrad Stab 2008; 93:1205–13.
[208] Staggs JEJ. Simple mathematical models of char-forming polymers. Polym Int 2000;49:1147–52.
[209] Staggs JEJ. Short communication: approximate solutions for the pyrolysis of char forming and filled polymers under thermally thick conditions. Fire Mater 2000;24:305–8.